Cell group architecture dictates phage exposure in multispecies biofilms

James B. Winans[1], Benjamin R. Wucher[1], Carey D. Nadell[1]*

[1] Department of Biological Sciences, Dartmouth, Hanover, NH 03755

* Author for correspondence:

carey.d.nadell@dartmouth.edu
78 College St., Rm. 326
Dartmouth, Dept. of Biological Sciences
Hanover, NH 03755

Abstract

Numerous ecological interactions among microbes – for example, competition for space and resources, or interaction among phages and their bacterial hosts – are likely to occur simultaneously in multispecies biofilm communities. While biofilms formed by just a single species occur, multispecies biofilms are thought to be more typical of microbial communities in the natural environment. Previous work has shown that multispecies biofilms can increase, decrease, or have no measurable impact on phage exposure of a host bacterium living alongside another species that the phages cannot target. The reasons causing this variability are not well understood, and how phage-host encounters change within multispecies biofilms remains mostly unexplored at the cellular spatial scale. Here, we explore how the microscale biofilm structure of a model 2-species biofilms impacts cell-cell and cell-phage interactions underlying larger population wide patterns. Our system consists of dual-culture biofilms of *Escherichia coli* and *Vibrio cholerae* under exposure to T7 phages or λ phages. In the absence of phages, the two species compete with each other for limited space and resources. As shown previously, sufficiently mature biofilms of *E. coli* can protect themselves from phage exposure via their curli matrix. Before this stage of biofilm structural maturity, *E. coli* is highly susceptible to phages, however we show that these bacteria can gain lasting protection against phage exposure if they have become embedded within highly packed groups of *V. cholerae* in co-culture. In this manner, *E. coli* cells that are otherwise susceptible to T7 and λ phages can survive phage exposure in the absence of *de novo* resistance evolution. While co-culture growth allows for earlier protection from phages conferred by *V. cholerae* cells, it comes at the cost of competing with *V. cholerae* and a disruption of normal curli-mediated protection for *E. coli* even in dual species biofilms grown over long time scales.

Introduction

Many organisms find refuge from threats within groups. This observation applies across scales from migrating bird flocks and animal herds to fish schools and insect swarms[1,2]. Bacteria are no exception and routinely live as collectives either free-floating or adhered to surfaces. Usually termed biofilms, these bacterial communities are abundant in natural settings[3–10], as are the threats faced by biofilm-dwelling microbes, such as invading competitors[11,12], diffusible antimicrobial compounds[13], phages[14,15], and predatory bacteria[16–18]. While biofilms formed by just a single species do occur, multispecies biofilms are thought to be more typical of microbial communities in the natural environment[19–22]. How microbial ecology might change within multispecies biofilms is not well known, including phage-host encounters, which remain mostly unexplored at the cellular spatial scale of interactions that underlie large scale patterns in biofilm-dominated microbial communities.

Previous work has shown that dual species biofilm cultures can increase, decrease, or have no measurable effect on phage susceptibility of a target host species living alongside a different, phage-resistant species[23–31]. Why do some dual species biofilms confer increased phage protection to susceptible host bacteria, while others appear to do the opposite? The details underlying this variability in outcome are not well understood. A common feature among many previous studies on this topic is the use of bulk assay CFU and PFU plating techniques from microtiter dish cultures; these tools, while highly effective for experimental throughput, by their nature provide an average result over entire biofilm populations residing on microtiter well walls. The conditions within these wells – for example, as a function of distance from the air-liquid interface – can vary substantially. An important way to expand on the foundation set by prior work is to examine the microscale variability in biofilm structure that can clarify the cell-cell and cell-phage interactions giving rise to community-wide patterns at larger spatial scales. In this paper we target this less-explored element of phage-host interaction in multispecies contexts.

Our model system comprises dual-culture biofilms of *Escherichia coli* and *Vibrio cholerae* under exposure to T7 phages or λ phages. Beyond the experimental tractability that makes *E. coli* and *V. cholerae* excellent for controlled experiments, these species can be found in natural environments together: for example, residing in brackish water[32,33] and within surface-fouling biofilms in coastal waters near human populations[34]. Members of the *Escherichia* and *Vibrio* genera are also common components of zebrafish microbiota[35,36]. The cellular arrangement and secreted matrix architectures of *V. cholerae* have been explored in great detail in the last decade[37–47]. In *V. cholerae,* biofilm structure is characterized by tight cell packing coordinated by four matrix components: the proteins RbmA, RbmC, Bap1, and the core polysaccharide VPS[46]. *E. coli* biofilms, likewise, have been dissected extensively[48–52]. T7 phage, belonging to the *Podoviridae* family, is an obligately lytic phage that is routinely isolated from the environment alongside *E. coli*[53]. T7 was used as our primary model phage, but we also performed similar experiments with temperate phage λ of the *Myoviridae* family to explore the generality of our results.

Recent work has documented protection of biofilm-dwelling bacteria against phage exposure among several species, including *V. cholerae*, *E. coli*, *Pseudomonas aeruginosa*, and *Pantoea stewartii*[41,54–56]. In each of these cases phage protection has either been directly or indirectly traced to biofilm architecture controlled by secreted matrix materials. Most pertinently, recent work in *E. coli* has shown that mature biofilms are able to block phage diffusion in a manner dependent on secreted curli polymers controlling cell-cell packing on the biofilm periphery[49,54]. Phages trapped in the outer biofilm layers remain at least partially viable and can infect newly arriving susceptible bacteria colonizing the biofilm exterior[57]. In general, there is little known about how growing in a multispecies context alters

biofilm matrix production and architecture relative to that found in monospecies contexts; likewise, there is little known about whether and how these potential changes in biofilm microscale structure influence the ability of phages to access their hosts.

Here we explore these open questions, studying how co-culture with *V. cholerae* influences matrix secretion and biofilm architecture of *E. coli*, and how these changes in turn influence the ability of *E. coli* to protect itself from phage attack in the midst of competition with *V. cholerae* for space and resources. We find that the patterns of phage infection among *E. coli* are substantially affected by the presence of a competing species, depending on microscale cell group spatial structure.

Results and Discussion

E. coli embedded in *V. cholerae* cell clusters are shielded from phage exposure

V. cholerae and *E. coli* were engineered to constitutively produce the fluorescent proteins mKO-κ and mKate2, such that they could be distinguished by fluorescence microscopy. We note that the strain background of *V. cholerae* that we use here, El Tor N16961, does not antagonize *E. coli* via Type VI secretion activity in these culture conditions[58,59]. The two species were inoculated at a 2:1 ratio of *V. cholerae* and *E. coli* into microfluidic devices bonded to glass coverslips, allowed to attach to the glass surface for 45 min, and then incubated under continuous flow of M9 minimal medium with 0.5% glucose for 48 h. Within this timeframe, biofilms begin to form, however monoculture *E. coli* biofilms have not yet produced sufficient curli matrix to prevent phage entry. T7 phages were then introduced to the system continuously at 10^4 per µL for 16 h; this strain of T7 contains a reporter construct causing infected hosts to produce sfGFP prior to lysis[54]. Changes in *E. coli* abundance and localization in the chamber were tracked and compared to those in equivalent biofilms without phage introduction.

Prior to phage introduction, we noted considerable variation in microscale biofilm structure and composition. Depending on the initial surface distribution of *V. cholerae* and *E. coli*, different regions of the devices contained cell groups of *E. coli* mostly on its own, locally mixed with *V. cholerae,* or occasionally embedded in the bottom layers of highly packed, *V.* cholerae-dominated clusters. Shortly after phage introduction, most *E. coli* cells growing on their own quickly began reporting infection and then lysed (Fig1A, SI Videos 1&2). Over the next 16 h, *E. coli* cells embedded within *V. cholerae*-dominated cell groups largely survived phage exposure, with scattered singleton *E. coli* cells elsewhere in the chambers. These single cells persisted for as long as we continued to track the system (up to 144 h) but did not appear to be actively replicating, or any new cells derived from them did not remain in place. After 16 h, waves of T7 infection could be seen proceeding partially into groups of *E. coli* embedded within *V. cholerae* biofilms, but a fraction of *E. coli* most often survived (Figure 1A).

To determine if the remaining *E. coli* survived because of *de novo* evolution of resistance to T7, we performed runs of this experiment after which all *E. coli* cells in the chamber were dispersed by agitation and tested for T7 resistance (see Methods). The frequency of T7 resistance in the surviving *E. coli* population was 10^{-5}, roughly the same as the frequency of resistance prior to the introduction of T7 phages[60]. This outcome shows that there was little or no substantive population compositional shift due to selection for *de novo* phage resistance (SI Figure S1C). This is not particularly surprising, as the host and phage population sizes – and, most importantly, the extent of movement and contact events between hosts and phages – are dramatically lower in these experiments compared to those that are typical in well-mixed batch culture. Rather, these experiments suggest that T7-susceptible *E. coli* survives phage introduction in our biofilm culture conditions by avoiding direct exposure to them entirely when embedded in groups of *V. cholerae*. We confirmed that this outcome is specific to the biofilm context by replicating

the same experiment in shaken liquid culture beginning with the same cell inoculum and phages introduced at equivalent multiplicity of infection (see Methods). In liquid culture conditions, T7-susceptible *E. coli* gained no protection against phage exposure and infection (SI Figure S1D). In the biofilm context, the delay between the start of biofilm growth and phage introduction was important for the experimental outcome; if phages were introduced from the beginning of biofilm growth, rather than 48 h after biofilm growth, then the extent of *E. coli* protection was all but eliminated (SI Figure S2).

Our observations above suggested that in dual-species culture conditions, the majority of *E. coli* that survive phage introduction are the cells enveloped within densely packed *V. cholerae* clusters. To test this idea quantitatively[16,61], We segmented and merged the cell volumes of *E. coli* and *V. cholerae* to calculate the joint neighborhood cell packing density for the two species throughout the imaged 3-D space (Fig 1B). By visual inspection, regions in which *E. coli* survived contained a majority of *V. cholerae* and had relatively high cell packing (biovolume fraction > 0.9), in comparison with other regions where *E. coli* tended to die of phage exposure and cell packing was lower (biovolume fraction = 0.3-0.6). We next measured the spatial association of *V. cholerae* with *E. coli* to see how this may change in the presence versus the absence of phage exposure. For this measurement we segmented the *E. coli* population away from background, and then measured *V. cholerae* fluorescence in direct proximity within 2μm of *E. coli* throughout all replicates with or without phages introduced. Compared to control experiments with no phages (Fig 1C), *V. cholerae* fluorescence was indeed significantly elevated in close proximity to *E. coli* after phage exposure, representing the surviving, protected portion of the *E. coli* population embedded within groups of *V. cholerae*. This protection effect could be replicated when introducing λ phages instead of T7 phages (SI Figure S3), and in a parallel study we show that the same effect occurs under predation by the bacterium *B. bacteriovorus* (Wucher et al., 2022, *bioRxiv*)[62].

At the scale of the entire chamber community, *E. coli* showed higher survival in co-culture with *V. cholerae* than in monoculture on its own (Fig 1D). In absolute terms, the total population size of *E. coli* after phage exposure in co-culture with *V. cholerae* was not statistically different from the surviving population size after phage exposure in *E. coli* monoculture (Fig 1E). This result occurred because *E. coli* total abundance prior to phage introduction is lower in co-culture with *V. cholerae*, with which it is competing for space and nutrient resources, but due to embedding of many *E. coli* cells within *V. cholerae* clusters, their per-cell survival rate against phage exposure is substantially higher relative to a *E. coli* monoculture condition (Figure 1D). So, on short time scales after phage introduction, there is a significant increase in survival rate for *E. coli* growing in co-culture with *V. cholerae*, but not yet a significant difference in the absolute abundance of surviving *E. coli*. However, we note another important difference between the *E. coli* that survive within *V. cholerae* colonies and those that survive in *E. coli* monoculture: the former cells maintain positive net growth within *V. cholerae* colonies and recover from the initial population decline, whereas the latter do not. We elaborate on this point with longer time-scale experiments in the last Results section.

Protection within *V. cholerae* cell clusters depends on their packing structure

After demonstrating that *E. coli* cells have reduced exposure to phages when embedded in clusters of *V. cholerae*, we explored the biofilm architectural features needed for protection to occur. As we have found previously that the extent of *V. cholerae* cell-cell packing can influence transport of phages and bacteria through biofilms, our first hypothesis based on prior work was that the high-density cell packing of *V. cholerae* biofilms was important for this protection mechanism[11,16,41]. Our other hypothesis, not mutually exclusive, was that phages may be sequestered away from *E. coli* by irreversible attachment to the

surface of *V. cholerae* cells in close proximity. To distinguish between these mechanisms, or to estimate their relative contribution to *E. coli* protection within *V. cholerae* clusters, we performed new experiments manipulating *V. cholerae* cell packing in co-culture with *E. coli* and assessing the degree of attachment and neutralization of T7 phages on the surface of *V. cholerae.*

To alter *V. cholerae* cell packing structure, we performed co-culture experiments similar to those in the previous section, but using a strain of *V. cholerae* (denoted Δ*rbmA*) with a clean deletion of the *rbmA* locus. This strain cannot produce the matrix protein RbmA, which is not essential for biofilm formation but is necessary for the tight cell packing that is characteristic of mature *V. cholerae* biofilms (SI Fig S4)[44,47,63]. Biofilms without RbmA, in contrast with those of WT, have previously shown to be permeable to vibrio phages, to planktonic competitor bacteria, and to predatory bacteria such as *Bdellovibrio bacteriovorous*[11,16]. If the high cell packing to which RbmA contributes is important to the protection of *E. coli* from phage exposure*,* we expect that in co-culture biofilms with Δ*rbmA V. cholerae*, *E. coli* will be more exposed to T7 phage predation and show different population dynamics relative to control co-cultures with WT *V. cholerae*.

We grew *E. coli* and Δ*rbmA V. cholerae* in biofilm co-culture, introduced T7 phages after 48 h as above, and found that the *E. coli* grown in the presence of Δ*rbmA V. cholerae* does not exhibit population recovery after phage introduction as it does in co-culture with WT *V. cholerae* (Fig 2A). This outcome suggests that *E. coli* does not gain protection from phage exposure amidst Δ*rbmA V. cholerae*, and that the cell packing architecture of WT *V. cholerae* is in fact important for this protection effect. If *E. coli* is protected within WT *V. cholerae* clusters, but not within Δ*rbmA* clusters, then in a tri-culture experiment of *E. coli*, Δ*rbmA V. cholerae*, and WT *V. cholerae*, we expect a shift of *E. coli* spatial association toward WT *V. cholerae* after introducing phages as *E. coli* associated with Δ*rbmA V. cholerae* are more often killed. We performed this tri-culture experiment, measuring the average distance between *E. coli* and WT *V. cholerae,* and that between *E. coli* and Δ*rbmA V. cholerae,* before and after phage introduction. Without the addition of phages into the triculture condition, *E. coli* cells are just as likely to be associated with WT *V. cholerae* (median distance: .88 μm) as they are with Δ*rbmA V. cholerae* (median distance: .69 μm) (Fig 2B and 2C). When phages are introduced, the remaining *E. coli* were significantly closer to WT *V. cholerae* (median distance: 0.59 μm) than they were to Δ*rbmA V. cholerae* (median distance: 3.46 μm) (Fig 2B).

The experiments above indicate that the packing architecture of WT *V. cholerae* biofilms is important for phage exposure protection of *E. coli* within them, as *E. coli* gains little if any protection from phage exposure in proximity to loosely packed Δ*rbmA V. cholerae*. These data do not exclude the possibility that this difference is due in part to sequestration of phages by attachment to *V. cholerae* cells, which could occur more often in WT clusters with higher density of available *V. cholerae* cell surface relative to clusters of the Δ*rbmA* strain. To help assess whether sequestration of phages by direct attachment to *V. cholerae* cell surface was important, we incubated *V. cholerae, E. coli*, and Δ*trxA E. coli* with T7 phages in shaken liquid culture, tracking the ability to recover T7 phages every 5 min for 1h (Fig 3E). In addition to a blank media control, the Δ*trxA E. coli* strain was included because this strain can adsorb phages normally but undergoes abortive infection, preventing phage amplification[64]. As expected, with Δ*trxA E. coli* incubation T7 PFU recovery steadily decreased until saturation at 1h. Incubated with WT *E. coli*, T7 PFU recovery initially decreased as phage adsorption occurred, followed by a rapid increase as new phages were released. Another round of latency and amplification then occurred before the 1h stop time. Incubated with *V. cholerae*, no change in T7 PFU recovery was observed, which was

identical to the blank media control for the duration of the experiment. These data suggest that T7 phages are not sequestered by adsorption to the *V. cholerae* cell surface.

Though T7 phages do not appear to adhere to *V. cholerae* cell surface, within biofilm cell clusters *V. cholerae* surface properties may differ, and they are also embedded in matrix polysaccharide and protein components. With this in mind we also performed experiments with fluorescently labeled T7 phages in biofilm growth conditions to determine if T7 is sequestered to *V. cholerae* cell groups in this context. Labeled phages were introduced to *V. cholerae* and *E. coli* dual culture biofilms and tracked over time, and we found that they localize strongly to unprotected *E. coli* cells, and not to *V. cholerae* (SI Fig S5). When *V. cholerae* monoculture biofilms were grown in flow devices with labeled phages added continuously in the media, we saw no accumulation of phages along the outer surface of *V. cholerae* cell clusters (SI Fig S6). We found occasional phages within *V. cholerae cell* groups along the basal glass substrate, but not in the rest of their interior volume (SI Fig. S6). As phages were added from the beginning of biofilm growth onward in this experiment, the results suggest that *V. cholerae* biofilm colonies expanded over the top of initially glass-attached phages, rather than phages diffusing through biofilms to the basal layer.

Taken all together, the data in the experiments above suggest that *E. coli* is unexposed to phages within WT *V. cholerae* biofilms due to their architectural features, with minimal if any sequestration of phages by direct adsorption to the surface of *V. cholerae* cells.

Cohabitation with *V. cholerae* alters *E. coli* matrix production

As noted in the first Results section, *E. coli* accumulates less quickly in co-culture with *V. cholerae* than it does on its own, owing to competition for limited space and resources. Previous work has shown that, in monoculture, *E. coli* biofilms can protect themselves against phages once they begin to produce curli matrix proteins, which interrupt phage binding on the single cell scale and contribute to biofilm architecture that blocks phage diffusion on the collective cell scale[54]. Curli production does not usually start until several days after beginning *E.* coli biofilm growth in microfluidic culture conditions[54], and we wondered if growing together with and competing against *V. cholerae* in dual culture might delay or disrupt curli formation. We note again that in the experiments in previous sections, biofilms were cultivated for too short a time for *E. coli* to begin producing curli matrix even in monoculture conditions. Here we explored whether co-culture with *V. cholerae* impacts curli production on longer time scales, when *E. coli* on its own would ordinarily be able to protect itself against phage exposure via curli production.

If curli production is reduced or disrupted by growth with *V. cholerae* as a competitor, we would expect no difference in phage exposure survival between WT *E. coli* and a strain lacking curli matrix in co-culture with *V. cholerae*. To explore this possibility, WT *E. coli* and an isogenic curli null deletion strain (denoted Δ*csgA*) were grown either on their own or in co-culture with *V. cholerae* for 96 h. This cultivation period is twice as long as is normally required for monoculture WT *E. coli* biofilms to produce curli and block phage diffusion. Biofilms were imaged at 96 h, exposed to phages at 10^4 per μL under 0.1 μL/min flow for 16 h, and then imaged again to document population sizes of WT and Δ*csgA E. coli* before and after phage introduction. As expected, the WT *E. coli* monoculture biofilms had the highest level of survival, with some replicates showing net increases in population size after the 16 h phage treatment. *E. coli* Δ*csgA* monoculture biofilms, lacking any protection mechanism against phage exposure, had the lowest level of survival. In contrast, when in co-culture with *V. cholerae*, WT *E. coli* and Δ*csgA E. coli*

(Figure 3A) showed no difference in survival to phage exposure, suggesting that curli production is no longer critical to T7 exposure protection for WT *E. coli* in this context.

To assess why curli-based phage protection was no longer operating for *E. coli* even in co-culture biofilms that had grown over 96 h, we repeated the experiments above with an WT *E. coli* strain harboring reporter fusions for monitoring *csgBAC* transcription and curli protein production. The transcriptional reporter was made previously by introducing *mKate2* in single copy on the chromosome within the *csgBAC* operon encoding two subunits of curli fiber protein (CsgB baseplate and CsgA primary curli monomer) and CsgC, which inhibits improper aggregation of CsgA monomers[54]. The protein production reporter was also made previously by introducing a 6x-His fusion tag to *csgA*, which allowed for *in situ* immunostaining of curli fibers produced by *E. coli* during growth in monoculture and co-culture with *V. cholerae*. As noted previously the total population size of *E. coli* in biofilms with *V. cholerae* is lower than that found in monoculture (Figure 3B, E-F). On a per cell basis over the entire chambers, *csgBAC* transcription and curli immunostaining were significantly higher for *E. coli* growing alone versus *E. coli* growing in co-culture with *V. cholerae* (Figure 3C-D). These patterns manifested at the scale of the whole chamber; on a smaller spatial scale, *E. coli* distance from *V. cholerae* in co-culture was not correlated with curli production (Figure SI S7).

Overall, these results suggest that *E. coli* curli production is substantially reduced when growing together with *V. cholerae*. It is not clear exactly why this is the case, but we speculate here that co-culture with *V. cholerae* alters one or a combination of nutrient availability, microenvironment osmolarity, and envelope stress experienced by *E. coli*, all of which influence the regulation of curli production[52]. The reduction in curli production may in turn contribute to the loss of curli based protection against T7 phages even after long incubation periods over which *E. coli* normally develops curli-based phage protection in monoculture. Together with the previous section our experiments here also indicate that while *E. coli* has a lower ability to protect itself via curli matrix production when in co-culture, it can avoid phage exposure altogether within *V. cholerae* colonies.

Ecological consequences joint interspecific competition and phage exposure

Our results thus far indicate complex ecological dynamics in which *E. coli* suffers a fitness reduction in exploitative competition with *V. cholerae*, but on the other hand *E. coli* can gain protective fitness benefit against phage exposure when embedded in the highly packed biofilm cell clusters that *V. cholerae* produces. It is still not clear, though, whether this protection is lasting under prolonged phage exposure, or whether *E. coli* remains viable within *V. cholerae* clusters despite being packed into their bottom-most cell layers. To characterize these population dynamics more thoroughly, we performed new experiments in which *E. coli* and *V. cholerae* were inoculated alone or together and grown for 48 h, followed by either continuous phage exposure or no phage exposure for an additional 96 h. (Figure 4). Note that this experimental regime is such that even in monoculture, *E. coli* will not have produced sufficient curli to block phage diffusion at the onset of phage influx into the biofilm chambers.

The population dynamics of *E. coli* and *V. cholerae* without T7 addition confirm our earlier suggestion that this interaction is competitive by default; *E. coli* population size is reduced in co-culture relative to when growing on its own (Figure 4E; yellow versus grey square trajectories). *V. cholerae* total productivity is also reduced in co-culture with *E. coli* relative to when growing on its own (Figure 4F), though overall it outcompetes *E. coli* by a substantial margin (Figure S8). This result was driven by *V. cholerae* biofilm clusters expanding more rapidly and robustly in lateral and vertical space, displacing some neighboring *E. coli* and enveloping other *E. coli* cell groups along the glass surface (Figure 4B).

Under prolonged phage exposure, however, these same enveloped clusters remain mostly protected from phage killing. We did observe occasional *E. coli* deaths within trapped clusters, shown via the T7 infection reporter (Figure 4C,D), but overall the *E. coli* cell groups maintained positive net growth and expanded laterally as the overlaid *V. cholerae* biofilms expanded as well (Figure 4E). Based on our earlier experiments, we suspect that progeny phages released from these occasional infection events within protected clusters were mostly trapped in place, and a sufficient impedance to phage diffusion will allow for long term survival of phage-susceptible hosts in close proximity[54,65]. Though we have linked *V. cholerae* cell packing to this phage diffusion limitation, the exact biophysical explanation for limited phage diffusion is an important future question. We speculate here that high density packing of *V. cholerae*, combined with the biochemical properties of its matrix and potentially sequestration of phages to trapped debris from lysed *E. coli*, may all contribute to the impeded diffusion of T7 phages from initial sites of infection and amplification.

Given that monoculture *E. coli* biofilms have a lower cell packing density than *V. cholerae* biofilms (Figure S9), and that the inclusions of *E. coli* within the *V. cholerae* biofilms continue expanding through time, we were curious to see if *E. coli* cell groups trapped within *V. cholerae* biofilms interrupted their highly packed structure. We assessed this question by calculating their two species' joint neighborhood cell packing, finding it to be stable over time and indistinguishable from what *V. cholerae* produces on its own. This suggests that the *V. cholerae* biofilm architecture, once initiated, can force cell groups of other species trapped within them into high packing orientations that do not disrupt the overall structure (SI Fig S9)[40,43,66,67]. As we explored in a parallel study on *B. bacteriovorus* predation in dual species biofilms, co-culture with *E. coli* only disrupts *V. cholerae* architecture when cells of both species begin dividing directly adjacent to each other from the outset of biofilm growth (Wucher et al., 2022, *bioRxiv*)[62].

From an ecological point of view, the net result of these architectural details is that if phage exposure occurs before *E. coli* is able to produce protective curli matrix, *E. coli* has higher absolute fitness in co-culture with *V. cholerae* – with which it is otherwise competing – than it does on its own (Figure 4C, yellow versus grey circles). The same process of envelopment of *E. coli* by expanding *V. cholerae* biofilms, which in the absence of phages reduces *E. coli* population growth relative to monoculture, protects *E. coli* from near total population collapse when phages are present. Since *V. cholerae* still has somewhat reduced absolute fitness in co-culture with *E. coli* compared to monoculture (regardless of phage addition; SI Figure S8), this interaction can be characterized as *E. coli* parasitizing or exploiting *V. cholerae* biofilm structure and gaining some protection at their expense in the presence of *E. coli*-targeting phages.

Conclusion

How microscale spatial structure in biofilms influences bacterial community ecology, and vice versa, are an important questions in microbial ecology benefiting from recent advances in live microscopy and image analysis[22,61,68–70]. Here we have explored the spatial population dynamics of *E. coli* cohabiting biofilms with *V. cholerae*, asking in particular how this 2-species system influences the interaction between *E. coli* and the lytic phage T7. *E. coli* biofilms can self-protect against T7 phage exposure by producing curli matrix, but before producing curli, *E. coli* biofilms are highly vulnerable to phages. When otherwise *E. coli* populations would collapse due to T7-mediated killing, it benefits from biofilm co-habitation with *V. cholerae* because pockets of *E. coli* become enveloped within densely packed *V. cholerae* colonies that strongly reduce phage diffusion. We identified the packing structure of *V. cholerae* biofilms as essential to T7 phage blocking, as has been implied previously for *Vibrio* phages as well[41].

There may be other contributions toward phage blocking from the electrostatic and hydrophobicity properties of *V. cholerae* biofilm matrix, which are notable questions for future work. We also showed that *E. coli* matrix production is altered in longer term biofilm co-culture with *V. cholerae*, with which, by default, *E. coli* competes for space and resources. Interestingly, with phages introduced to the system this relationship becomes exploitative on the part of *E. coli*, which gains protection from phage exposure while taking up space that *V. cholerae* could ordinarily occupy within the highly-packed cell groups that it produces. Broadly speaking, the molecular mechanisms underlying differences between multispecies and single species biofilm architectures remains underexplored and will provide important ground for future work.

Prior literature has documented that co-habiting biofilms with other species can render bacteria more, less, or equally susceptible to phage attack in comparison to when growing in single species conditions under phage exposure[31] . Our experiments here document that all of these outcomes can occur within the same system occupying less than 1mm^2, depending on the microscale biofilm architecture of the two species and the timing of biofilm growth before exposure to phages. For example, in biofilms grown for less time that *E. coli* needs to produce curli matrix and protect itself from phages, co-culture with *V. cholerae* leads to increased phage protection where *E. coli* becomes embedded within *V. cholerae* clusters; but there is no change in vulnerability where *E. coli* grows in clusters just outside the periphery of tightly packed *V. cholerae* groups (Figure 1). On the other hand, in biofilms grown for longer periods over which *E. coli* would normally protect itself via curli production on its own, co-culture with *V. cholerae* leads to reduced curli production and reduced protection from phage exposure for any *E. coli* not embedded in *V. cholerae* cell clusters (Figure 3). We envision that examining other systems of multi-host, multi-phage composition at this level of spatial detail will reveal similarly complex dependencies of community dynamics on the nature of cell group architecture and the time scales of community growth versus phage exposure.

How spatial constraints influence community ecology has gained momentum as an important frontier in microbiology research as we try to relate the massive amount of sequencing data on community composition in myriad environments to the microscale processes of multispecies interaction[21,22,71–73]. This study examines what is possible when two species that construct biofilms with different combinations of cell growth pattern and matrix composition interact together under phage exposure for one of the bacterial biofilm-dwellers. Future work will benefit from ever increasing realism in the species composition and environmental features in which the many elements of biofilm ecology can be explored.

Acknowledgements

We are grateful to William Harcombe, Mary Lou Guerinot, and Alexandre Persat for feedback on earlier versions of this manuscript, and to members of the Nadell Lab at Dartmouth for feedback on the project. We are very grateful as well to Lanying Zeng for generously providing phage λ*D-mNeongreen cI$_{857}$-mKate2* used for SI Figure 3. JBW is supported by a GAANN Fellowship from Department of Biological Sciences at Dartmouth. BRW is supported by a Gillman Fellowship from the Department of Biological Sciences at Dartmouth. CDN is supported by the Simons Foundation award number 826672, NSF grant IOS 2017879, NSF grant MCB 1817352, and grant RGY0077/2020 from the Human Frontier Science Program.

Author contributions

James B. Winans: Conceptualization, Resources, Data acquisition, Data curation, Formal analysis, Validation, Investigation, Visualization, Methodology, Writing – original draft, Writing - review and editing

Benjamin R. Wucher: Conceptualization, Resources, Methodology

Carey D. Nadell: Conceptualization, Resources, Data curation, Formal analysis, Supervision, Funding acquisition, Validation, Investigation, Visualization, Methodology, Writing - original draft, Project administration, Writing - review and editing

Methods

Strains

Bacterial strains used in this study were produced using the lambda red protocol or through allelic exchange. Briefly, primers encoding regions of homology to the host genome were used to amplify fluorescent markers fused to resistance cassette markers. These PCR products were used to knock in the fluorescent marker and selected for with the respective resistance cassette[54,57]. *V. cholerae* alterations were made using suicide vector pKAS32 for allelic exchange or pBW1 for SacB counter selection for allelic exchange[41,74]. Recombinant T7 phages were created by using T7select415-1 phage display system[54]. Recombinant λ phages were created by infecting *λDam cI$_{857}$ bor::KanR* phages on LE392 (permissive host) with plasmid pBR322-λD-mTurquoise2/mNeongreen-E for recombination, and further selection for fluorescent plaques[75].

Microfluidic flow device fabrication

Microfluidic chambers are produced by casting poly-dimethysiloxane (PDMS) onto preexisting chamber molds. The resulting PDMS blocks were cut to size, hole-punched for inlet and outlet channels then covalently bonded to #1.5 glass coverslips. The internal space of the chambers in which biofilms were cultivated measured 3000μm x 500μm x 70μm (LxWxH). Inlet tubing (Cole Parmer PTFE #30, inner diameter 0.3mm) affied to 25-guage needles on 1mL BD syringes were plumbed into chamber inlets, and the syringes were driven by Harvard Apparatus Pico Plus syringe pumps. Tubing from chamber outlet channels was fed to effluent collection dishes.

Biofilm culture conditions

Overnight cultures of *V. cholerae* and *E. coli* were inoculated into the microfluidic chambers at a ratio of 2:1. To achieve comparable amounts of biofilm growth in the *ΔrbmA V. cholerae*, WT *V. cholerae*, and *E. coli* triculture experiments, chambers were inoculated with a ratio of 6:3:1, respectively. After a 45-min incubation period without flow to allow for surface attachment, M9 minimal media with .5% glucose continuously flowed into the chamber at a rate of .1μL/min. For experiments with longer-term incubation to promote curli production by *E. coli* prior to phage introduction, and to discourage biofilm overgrowth of the chamber, chambers were incubated with M9 minimal media with .25% glucose.

For the immunostaining of curli, a new AR3110 strain harboring a translational 6xHis tag fused to *csgA*, which encodes the monomer for curli production, was stained with 6X His Tag Dylight 405 added

to the media at a concentration of .1µg/mL for the entirety of the experiment. Prior work has shown that addition of the 6xHis tag to CsgA does not interrupt its function by any measures tested[54]. For experiments investigating the effects of phage exposure, pairwise comparisons were made between flow devices of equal age that had phages added or did not have phages added, as the control for these experiments was the dynamics of co-culture growth without the presence of phage. For experiments investigating the disruption of curli matrix production, comparisons were made between flow devices before they experience phage exposure and after they experience phage exposure, as the control for these experiments were *E. coli* monoculture biofilms surviving exposure from phages. All experiments were carried out at room temperature.

Phage propagation, staining, and introduction to biofilms

T7 phages were produced by growing sensitive *E. coli* to OD_{600} = 0.4 in M9 minimal media with 0.5% glucose, before adding an aliquot of T7 phage and 200mM MgSO4 and incubating until the bacterial cultures were cleared. Phages were quantified using standard plaquing techniques, and back diluted to $1x10^4$/µL in M9 with .5% glucose. To visualize phage infection, we used a previously constructed T7 strain that induces sfGFP production by the host prior to lysis; to visualize phages directly, we stained T7 phages with Alexa Fluor™ 633 NHS Ester using the Phage on Tap protocol[76]. For experiments in which capsid-labeled phages were introduced to biofilms, the biofilms were grown for 48 h as described above, followed by continuous labeled phage addition at $5x10^6$/µL for the remainder of the experiment. λ phages were produced by growing lysogenic *E.* coli to an OD_{600} = 0.4 in M9 minimal media with 0.5% glucose, then heat shocked at 42Cº for 20 min, and then incubated at 37Cº until visible lysis occurred. For experiments with short phage exposure, phages were continuously introduced for 16 h. For experiments with extended phage exposure (Figure 4), phages were continuously added for 96 h. For the nascent biofilm phage exposures, phages were introduced into the chamber immediately following the initial attachment step. For the labeled phage timelapse, phages were added for a total of 20 h.

Biofilm dispersal and detection of *de novo* T7-resistance mutants from biofilm culture

V. cholerae and *E. coli* dual culture biofilms grown for 48 h and then treated with phages for 16 h were dispersed by removing the tubing from the microfluidic device and vigorously pipetting 100µL of M9 media and air bubbles back and forth between the inlet and outlet ports. This was done to ensure complete removal of all cells in the chamber in order to capture accurate measurements of total *E. coli* and *de novo* T7-resistant *E. coli*. To determine cell viability and phage sensitivity, this 100µL volume containing dispersed biofilm cells was serially diluted and plated on LB+50µg/mL kanamycin plates for total *E. coli* counts and, in parallel, on LB+50µg/mL kanamycin plates saturated with T7 phages to determine *de novo* T7-resistant counts. Kanamycin was added to selectively plate for *E. coli* and kill *V. cholerae*, as all *E. coli* strains carried a kanamycin resistance cassette on the chromosome from insertion of their constitutive fluorescent protein production constructs[54].

Dual liquid culture phage assay

5mL liquid dual cultures of room temperature M9 minimal media with 0.5% glucose were inoculated 2:1 with *V. cholerae* and *E. coli* each normalized to OD_{600} =0.15. 5µL samples of these dual cultures were taken at regular time intervals, serially diluted, and plated onto LB+50µg/mL kanamycin plates to obtain the CFU count for *E. coli.* At an OD_{600} measurement of 1.5, (15h), $6.5x10^7$ T7 phages were introduced to the dual cultures, as this is the estimated MOI in the biofilm condition. Note that MOI estimation is less

straightforward in biofilm culture, as many phages introduced by flow do not contact host cells and pass out of the chambers in the liquid effluent.

Phage adsorption assay

Bacterial cultures of *E. coli*, *E. coli* Δ*trxA*, and *V. cholerae* were grown and back-diluted to an OD_{600} = 0.5 in LB medium. T7 phages were added to a final concentration of $5x10^4$ phages per µL. Cultures were incubated at 37Cº and 500µL aliquots were taken every 5 min, passed through a .2µm filter, and stored on ice until the end of the experiment. The filtration step served to exclude any bacterial cells, and any phages that were attached to them, allowing us to measure phage association with cell material. Flowthrough samples were then serially diluted and plated for PFUs.

Microscopy and Image analysis

All imaging was performed using a Zeiss 880 line-scanning confocal microscope, using a 40x/1.2 N.A. water objective or a 10x/.4 N.A. water objective. The 6xHis Tag Antibody Dylight 405 that was used to stain 6xHis-tagged curli polymers was excited with a 405 laser line. The mTFP protein that *V. cholerae* produces in experiments investigating curli transcription was excited with the 458 laser line. The sfGFP protein produced by the T7 infection reporter construct, and the mNeonGreen capsid label of the λ phages were both excited (in separate experiments) with a 488 laser line. The mKO-κ protein that *V. cholerae* expresses constitutively and by *E. coli* that reports *csgBAC* transcription was excited with a 543 laser line (in separate experiments). The mKate2 protein that *E. coli* expresses constitutively and upon *csgBAC* transcription, and the mRuby2 protein that ΔcsgA *E. coli* constitutively expresses was excited with a 594 laser line (in separate experiments). The Alexafluor 647 conjugated onto the capsid of labeled T7 phage virions was excited with a 633 laser line. For each chamber in each experiment, multiple independent locations were chosen within each biofilm chamber and averaged to give one measurement for a given chamber in the case of whole-biofilm measurements. Prior to export, images were processed by constrained iterative deconvolution in ZEN blue.

Quantification and Statistics

All biofilm image quantification was performed within the BiofilmQ framework[61]. For 3D grid-based measurements detailing microscale architecture, segmented microbial volumes were divided into a 3D grid with each node 0.8µm on a side. Joint neighborhood cell packing measurements merged the biovolume of all bacteria within a sample and calculated the local biovolume fraction within 6µm of each segmented bacterial volume within each grid cube[16]. For experiments using λ phages, infection was measured by calculating a Mander's overlap coefficient between *E. coli* cells and λ phages. Mann-Whitney U-tests with the Bonferroni correction were used for pairwise comparisons.

Table 1. Bacterial and phage strains used in this study

Strain	**Relevant markers/Genotype**	**Source**
V. cholerae		
CNV 121	N16961, rbmA-3xFLAG, LacZ::Ptac-mKO-κ	[74]
CNV 126	N16961, *ΔrbmA*, LacZ::Ptac-mKo-κ	[41]
CNV 248	N16961, LacZ::Ptac mTFP	This study
E. coli		
CNE 320	AR3110, with ΔcsgA::scar, Ptac-mRuby2 and KanR inserted at attB site	[54]
CNE 336	AR3110, with csgBAC-mKate2 transcriptional fusion, Ptac-mKO-κ and KanR inserted at attB site	[54]
CNE 761	AR3110, *attB::mKate2-KanR*	[57]
CNE 772	AR3110, *attB::mKate2-KanR, ΔtrxA*	[57]
CNE 776	AR3110, *attB::mKate2-KanR, 6x-His csgA*	[57]
Phages		
CNX 9	WT phage T7	DSMZ (DSM4623)
CNX 11	T7 with sfGFP under control of phi 10 promoter	[54]
CNX 19	*λD-mNeongreen* cI_{857}*-mKate2 bor::*Cm^R	[75]

520

References

1. Couzin, I. D., Krause, J., James, R., Ruxton, G. D. & Franks, N. R. Collective Memory and Spatial Sorting in Animal Groups. *J. Theor. Biol.* **218**, 1–11 (2002).
2. Krause, J., Krause, P. of F. B. and E. J., Ruxton, G. D., Ruxton, G. & Ruxton, I. G. *Living in Groups*. (OUP Oxford, 2002).
3. Seneviratne, C. J., Zhang, C. F. & Samaranayake, L. P. Dental plaque biofilm in oral health and disease. *Chin. J. Dent. Res. Off. J. Sci. Sect. Chin. Stomatol. Assoc. CSA* **14**, 87–94 (2011).
4. Bjarnsholt, T. The role of bacterial biofilms in chronic infections. *APMIS. Suppl.* 1–51 (2013) doi:10.1111/apm.12099.
5. Passow, U., Ziervogel, K., Asper, V. & Diercks, A. Marine snow formation in the aftermath of the Deepwater Horizon oil spill in the Gulf of Mexico. *Environ. Res. Lett.* **7**, 035301 (2012).
6. Miranda, A. F. *et al.* Applications of microalgal biofilms for wastewater treatment and bioenergy production. *Biotechnol. Biofuels* **10**, 120 (2017).
7. Flemming, H.-C. *et al.* Biofilms: an emergent form of bacterial life. *Nat. Rev. Microbiol.* **14**, 563–575 (2016).
8. Flemming, H.-C. & Wingender, J. The biofilm matrix. *Nat. Rev. Microbiol.* **8**, 623–633 (2010).
9. Nadell, C. D., Xavier, J. B. & Foster, K. R. The sociobiology of biofilms. *FEMS Microbiol. Rev.* **33**, 206–224 (2009).
10. Katharios-Lanwermeyer, S. & O'Toole, G. A. Biofilm Maintenance as an Active Process: Evidence that Biofilms Work Hard to Stay Put. *J. Bacteriol.* **204**, e00587-21 (2022).
11. Nadell, C. D., Drescher, K., Wingreen, N. S. & Bassler, B. L. Extracellular matrix structure governs invasion resistance in bacterial biofilms. *ISME J.* **9**, 1700–1709 (2015).
12. Hibbing, M. E., Fuqua, C., Parsek, M. R. & Peterson, S. B. Bacterial competition: surviving and thriving in the microbial jungle. *Nat. Rev. Microbiol.* **8**, 15–25 (2010).
13. Stewart, P. S. Mechanisms of antibiotic resistance in bacterial biofilms. *Int. J. Med. Microbiol. IJMM* **292**, 107–113 (2002).
14. Hansen, M. F., Svenningsen, S. L., Røder, H. L., Middelboe, M. & Burmølle, M. Big Impact of the Tiny: Bacteriophage-Bacteria Interactions in Biofilms. *Trends Microbiol.* **27**, 739–752 (2019).
15. Pires, D. P., Melo, L. D. R. & Azeredo, J. Understanding the Complex Phage-Host Interactions in Biofilm Communities. *Annu. Rev. Virol.* **8**, 73–94 (2021).
16. Wucher, B. R., Elsayed, M., Adelman, J. S., Kadouri, D. E. & Nadell, C. D. Bacterial predation transforms the landscape and community assembly of biofilms. *Curr. Biol.* **31**, 2643-2651.e3 (2021).
17. Kadouri, D. & O'Toole, G. A. Susceptibility of biofilms to Bdellovibrio bacteriovorus attack. *Appl. Environ. Microbiol.* **71**, 4044–4051 (2005).
18. Mookherjee, A. & Jurkevitch, E. Interactions between Bdellovibrio and like organisms and bacteria in biofilms: beyond predator–prey dynamics. *Environ. Microbiol.* **24**, 998–1011 (2022).
19. Dar, S. A., Kuenen, J. G. & Muyzer, G. Nested PCR-Denaturing Gradient Gel Electrophoresis Approach To Determine the Diversity of Sulfate-Reducing Bacteria in Complex Microbial Communities. *Appl. Environ. Microbiol.* **71**, 2325–2330 (2005).
20. Elias, S. & Banin, E. Multi-species biofilms: living with friendly neighbors. *FEMS Microbiol. Rev.* **36**, 990–1004 (2012).
21. Borisy, G. G. & Valm, A. M. Spatial scale in analysis of the dental plaque microbiome. *Periodontol. 2000* **86**, 97–112 (2021).

22. Stacy, A., McNally, L., Darch, S. E., Brown, S. P. & Whiteley, M. The biogeography of polymicrobial infection. *Nat. Rev. Microbiol.* **14**, 93–105 (2016).
23. Harcombe, W. R. & Bull, J. J. Impact of Phages on Two-Species Bacterial Communities. *Appl. Environ. Microbiol.* **71**, 5254–5259 (2005).
24. González, S. *et al.* The Behavior of Staphylococcus aureus Dual-Species Biofilms Treated with Bacteriophage phiIPLA-RODI Depends on the Accompanying Microorganism. *Appl. Environ. Microbiol.* **83**, e02821-16 (2017).
25. Sillankorva, S., Neubauer, P. & Azeredo, J. Phage control of dual species biofilms of Pseudomonas fluorescens and Staphylococcus lentus. *Biofouling* **26**, 567–575 (2010).
26. Kay, M. K., Erwin, T. C., McLean, R. J. C. & Aron, G. M. Bacteriophage Ecology in Escherichia coli and Pseudomonas aeruginosa Mixed-Biofilm Communities. *Appl. Environ. Microbiol.* **77**, 821–829 (2011).
27. Tait, K., Skillman, L. C. & Sutherland, I. W. The efficacy of bacteriophage as a method of biofilm eradication. *Biofouling* **18**, 305–311 (2002).
28. Testa, S. *et al.* Spatial structure affects phage efficacy in infecting dual-strain biofilms of Pseudomonas aeruginosa. *Commun. Biol.* **2**, 1–12 (2019).
29. Abedon, S. T., Danis-Wlodarczyk, K. M., Wozniak, D. J. & Sullivan, M. B. Improving Phage-Biofilm In Vitro Experimentation. *Viruses* **13**, 1175 (2021).
30. Abedon, S. T. Bacteriophage-mediated biocontrol of wound infections, and ecological exploitation of biofilms by phages. in *Biofilm, Pilonidal Cysts and Sinuses* 121–158 (Springer, 2018).
31. Geredew Kifelew, L., Mitchell, J. G. & Speck, P. Mini-review: efficacy of lytic bacteriophages on multispecies biofilms. *Biofouling* **35**, 472–481 (2019).
32. Momtaz, H., Dehkordi, F. S., Rahimi, E. & Asgarifar, A. Detection of Escherichia coli, Salmonella species, and Vibrio cholerae in tap water and bottled drinking water in Isfahan, Iran. *BMC Public Health* **13**, 556 (2013).
33. Soleimani, F., Taherkhani, R., Dobaradaran, S., Spitz, J. & Saeedi, R. Molecular detection of E. coli and Vibrio cholerae in ballast water of commercial ships: a primary study along the Persian Gulf. *J. Environ. Health Sci. Eng.* **19**, 457–463 (2021).
34. Shikuma, N. J. & Hadfield, M. G. Marine biofilms on submerged surfaces are a reservoir for Escherichia coli and Vibrio cholerae. *Biofouling* **26**, 39–46 (2010).
35. Vargas, O. *et al.* Probiotic Yeasts and Vibrio anguillarum Infection Modify the Microbiome of Zebrafish Larvae. *Front. Microbiol.* **12**, (2021).
36. Rendueles, O. *et al.* A New Zebrafish Model of Oro-Intestinal Pathogen Colonization Reveals a Key Role for Adhesion in Protection by Probiotic Bacteria. *PLOS Pathog.* **8**, e1002815 (2012).
37. Qin, B. *et al.* Cell position fates and collective fountain flow in bacterial biofilms revealed by light-sheet microscopy. *Science* **369**, 71–77 (2020).
38. Zhang, Q. *et al.* Morphogenesis and cell ordering in confined bacterial biofilms. *Proc. Natl. Acad. Sci.* **118**, e2107107118 (2021).
39. Yan, J., Nadell, C. D., Stone, H. A., Wingreen, N. S. & Bassler, B. L. Extracellular-matrix-mediated osmotic pressure drives Vibrio cholerae biofilm expansion and cheater exclusion. *Nat. Commun.* **8**, 327 (2017).
40. Yan, J., Sharo, A. G., Stone, H. A., Wingreen, N. S. & Bassler, B. L. Vibrio cholerae biofilm growth program and architecture revealed by single-cell live imaging. *Proc. Natl. Acad. Sci.* **113**, E5337–E5343 (2016).

41. Díaz-Pascual, F. *et al.* Breakdown of Vibrio cholerae biofilm architecture induced by antibiotics disrupts community barrier function. *Nat. Microbiol.* **4**, 2136–2145 (2019).
42. Singh, P. K. *et al.* Vibrio cholerae combines individual and collective sensing to trigger biofilm dispersal. *Curr. Biol.* **27**, 3359–3366 (2017).
43. Drescher, K. *et al.* Architectural transitions in Vibrio cholerae biofilms at single-cell resolution. *Proc. Natl. Acad. Sci.* **113**, E2066–E2072 (2016).
44. Yildiz, F., Fong, J., Sadovskaya, I., Grard, T. & Vinogradov, E. Structural characterization of the extracellular polysaccharide from Vibrio cholerae O1 El-Tor. *PloS One* **9**, e86751 (2014).
45. Berk, V. *et al.* Molecular Architecture and Assembly Principles of Vibrio cholerae Biofilms. *Science* **337**, 236–239 (2012).
46. Teschler, J. K. *et al.* Living in the matrix: assembly and control of Vibrio cholerae biofilms. *Nat. Rev. Microbiol.* **13**, 255–268 (2015).
47. Fong, J. C. *et al.* Structural dynamics of RbmA governs plasticity of Vibrio cholerae biofilms. *eLife* **6**, e26163 (2017).
48. Serra, D. O., Richter, A. M. & Hengge, R. Cellulose as an Architectural Element in Spatially Structured Escherichia coli Biofilms. *J. Bacteriol.* **195**, 5540–5554 (2013).
49. Serra, D. O., Richter, A. M., Klauck, G., Mika, F. & Hengge, R. Microanatomy at Cellular Resolution and Spatial Order of Physiological Differentiation in a Bacterial Biofilm. *mBio* **4**, e00103-13.
50. Ziege, R. *et al.* Adaptation of Escherichia coli Biofilm Growth, Morphology, and Mechanical Properties to Substrate Water Content. *ACS Biomater. Sci. Eng.* **7**, 5315–5325 (2021).
51. Richter, A. M. *et al.* Local c-di-GMP Signaling in the Control of Synthesis of the E. coli Biofilm Exopolysaccharide pEtN-Cellulose. *J. Mol. Biol.* **432**, 4576–4595 (2020).
52. Serra, D. O. & Hengge, R. Bacterial Multicellularity: The Biology of Escherichia coli Building Large-Scale Biofilm Communities. *Annu. Rev. Microbiol.* **75**, 269–290 (2021).
53. Molineux, I. J. The T7 group. *The Bacteriophages* 277–301 (2006).
54. Vidakovic, L., Singh, P. K., Hartmann, R., Nadell, C. D. & Drescher, K. Dynamic biofilm architecture confers individual and collective mechanisms of viral protection. *Nat. Microbiol.* **3**, 26–31 (2018).
55. Dunsing, V., Irmscher, T., Barbirz, S. & Chiantia, S. Purely Polysaccharide-Based Biofilm Matrix Provides Size-Selective Diffusion Barriers for Nanoparticles and Bacteriophages. *Biomacromolecules* **20**, 3842–3854 (2019).
56. Darch, S. E. *et al.* Phage Inhibit Pathogen Dissemination by Targeting Bacterial Migrants in a Chronic Infection Model. *mBio* **8**, e00240-17 (2017).
57. Bond, M. C., Vidakovic, L., Singh, P. K., Drescher, K. & Nadell, C. D. Matrix-trapped viruses can prevent invasion of bacterial biofilms by colonizing cells. *eLife* **10**, e65355 (2021).
58. Bachmann, V. *et al.* Bile Salts Modulate the Mucin-Activated Type VI Secretion System of Pandemic Vibrio cholerae. *PLoS Negl. Trop. Dis.* **9**, e0004031 (2015).
59. Unterweger, D. *et al.* The Vibrio cholerae type VI secretion system employs diverse effector modules for intraspecific competition. *Nat. Commun.* **5**, 3549 (2014).
60. Simmons, E. L. *et al.* Biofilm Structure Promotes Coexistence of Phage-Resistant and Phage-Susceptible Bacteria. *mSystems* **5**, e00877-19 (2020).
61. Hartmann, R. *et al.* Quantitative image analysis of microbial communities with BiofilmQ. *Nat. Microbiol.* **6**, 151–156 (2021).

62. Wucher, B. R., Elsayed, M., Kadouri, D. E. & Nadell, C. D. Breakdown of cooperative architecture in dual species biofilms and the spatial ecology of predation. 2022.07.22.501146 Preprint at https://doi.org/10.1101/2022.07.22.501146 (2022).

63. Fong, J. C. N., Karplus, K., Schoolnik, G. K. & Yildiz, F. H. Identification and Characterization of RbmA, a Novel Protein Required for the Development of Rugose Colony Morphology and Biofilm Structure in Vibrio cholerae. *J. Bacteriol.* **188**, 1049–1059 (2006).

64. Bedford, E., Tabor, S. & Richardson, C. C. The thioredoxin binding domain of bacteriophage T7 DNA polymerase confers processivity on Escherichia coli DNA polymerase I. *Proc. Natl. Acad. Sci.* **94**, 479–484 (1997).

65. Simmons, M., Drescher, K., Nadell, C. D. & Bucci, V. Phage mobility is a core determinant of phage–bacteria coexistence in biofilms. *ISME J.* **12**, 531–543 (2018).

66. Nijjer, J. *et al.* Mechanical forces drive a reorientation cascade leading to biofilm self-patterning. *Nat. Commun.* **12**, 1–9 (2021).

67. Hartmann, R. *et al.* Emergence of three-dimensional order and structure in growing biofilms. *Nat. Phys.* **15**, 251–256 (2019).

68. Yanni, D., Márquez-Zacarías, P., Yunker, P. J. & Ratcliff, W. C. Drivers of spatial structure in social microbial communities. *Curr. Biol.* **29**, R545–R550 (2019).

69. Nadell, C. D., Drescher, K. & Foster, K. R. Spatial structure, cooperation and competition in biofilms. *Nat. Rev. Microbiol.* **14**, 589–600 (2016).

70. Jeckel, H. & Drescher, K. Advances and opportunities in image analysis of bacterial cells and communities. *FEMS Microbiol. Rev.* **45**, fuaa062 (2021).

71. Mark Welch, J. L., Rossetti, B. J., Rieken, C. W., Dewhirst, F. E. & Borisy, G. G. Biogeography of a human oral microbiome at the micron scale. *Proc. Natl. Acad. Sci.* **113**, E791–E800 (2016).

72. Sonnenburg, E. D. *et al.* Diet-induced extinctions in the gut microbiota compound over generations. *Nature* **529**, 212–215 (2016).

73. Dar, D., Dar, N., Cai, L. & Newman, D. K. Spatial transcriptomics of planktonic and sessile bacterial populations at single-cell resolution. *Science* **373**, eabi4882 (2021).

74. Wucher, B. R. *et al.* Vibrio cholerae filamentation promotes chitin surface attachment at the expense of competition in biofilms. *Proc. Natl. Acad. Sci.* **116**, 14216–14221 (2019).

75. Trinh, J. T., Székely, T., Shao, Q., Balázsi, G. & Zeng, L. Cell fate decisions emerge as phages cooperate or compete inside their host. *Nat. Commun.* **8**, 14341 (2017).

76. Bonilla, N. *et al.* Phage on tap-a quick and efficient protocol for the preparation of bacteriophage laboratory stocks. *PeerJ* **4**, e2261 (2016).

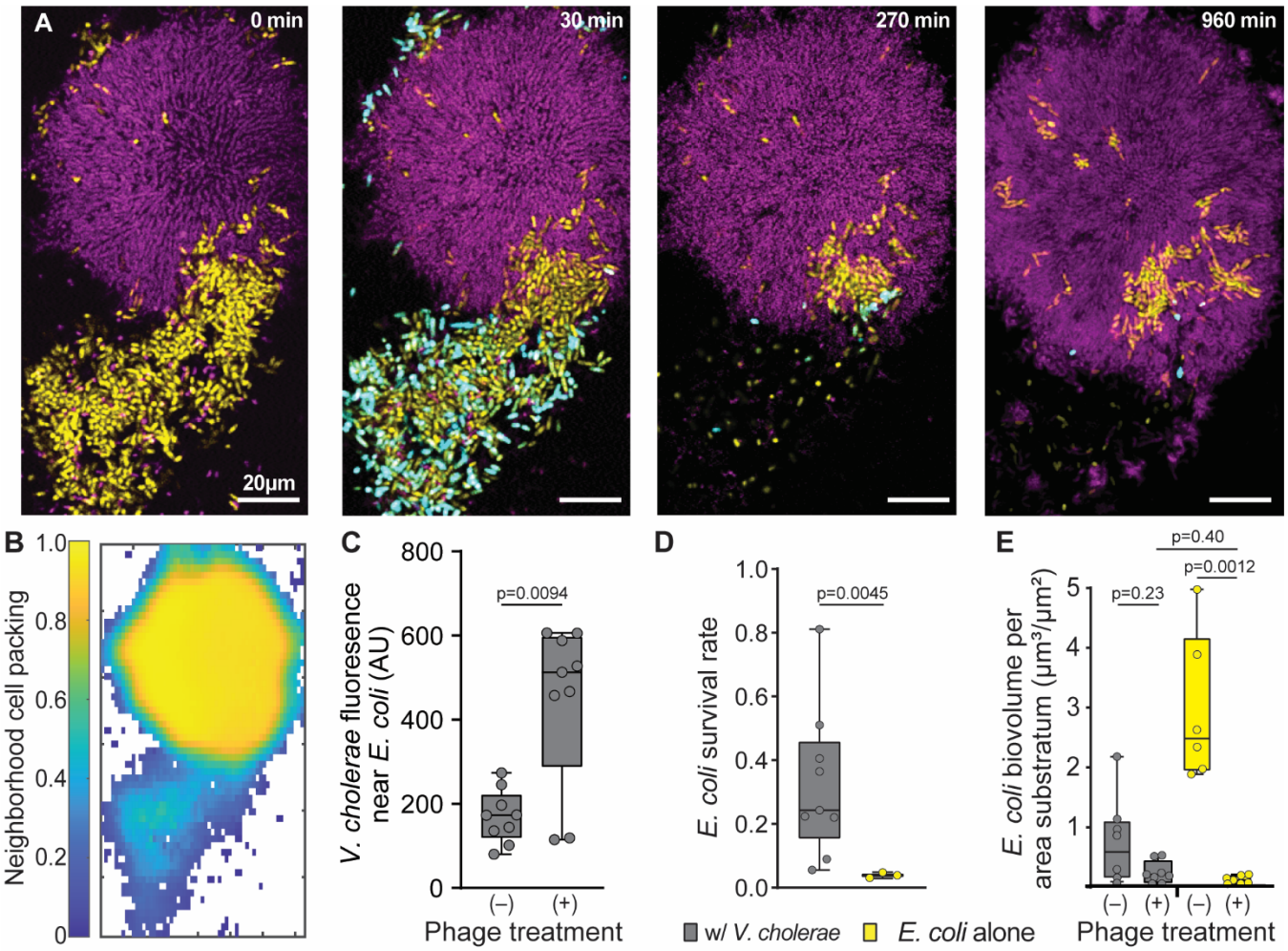

Figure 1. *E. coli* (yellow) embedded within *V. cholerae* cell groups can evade exposure to phages in the surrounding medium. **(A)** Timelapse series of a dual culture biofilm of *E. coli* (yellow) and *V. cholerae* (purple), undergoing T7 coliphage exposure (infected cells reporting in cyan/white). Time points noted in the upper right of each panel represent time since phage introduction was started. **(B)** The neighborhood biovolume fraction (biovolume fraction within a 6μm around each segmented bacterium) of the merged biovolumes of both *V. cholerae* and *E. coli* for the first time point in panel A. **(C)** Mean *V. cholerae* fluorescence signal found around *E. coli* cells in biofilms with and without phage exposure (Mann-Whitney U test with n=9). **(D)** *E. coli* biovolume normalized to biovolume prior to the introduction of phage in dual culture with *V. cholerae* and monoculture controls (Mann-Whitney U test with n=9, n=3). **(E)** Total biovolume of *E. coli* in dual culture and monoculture control biofilms with and without phage exposure at equivalent time points (Mann-Whitney U tests with n=8, n=9, n=6, n=7 from left to right).

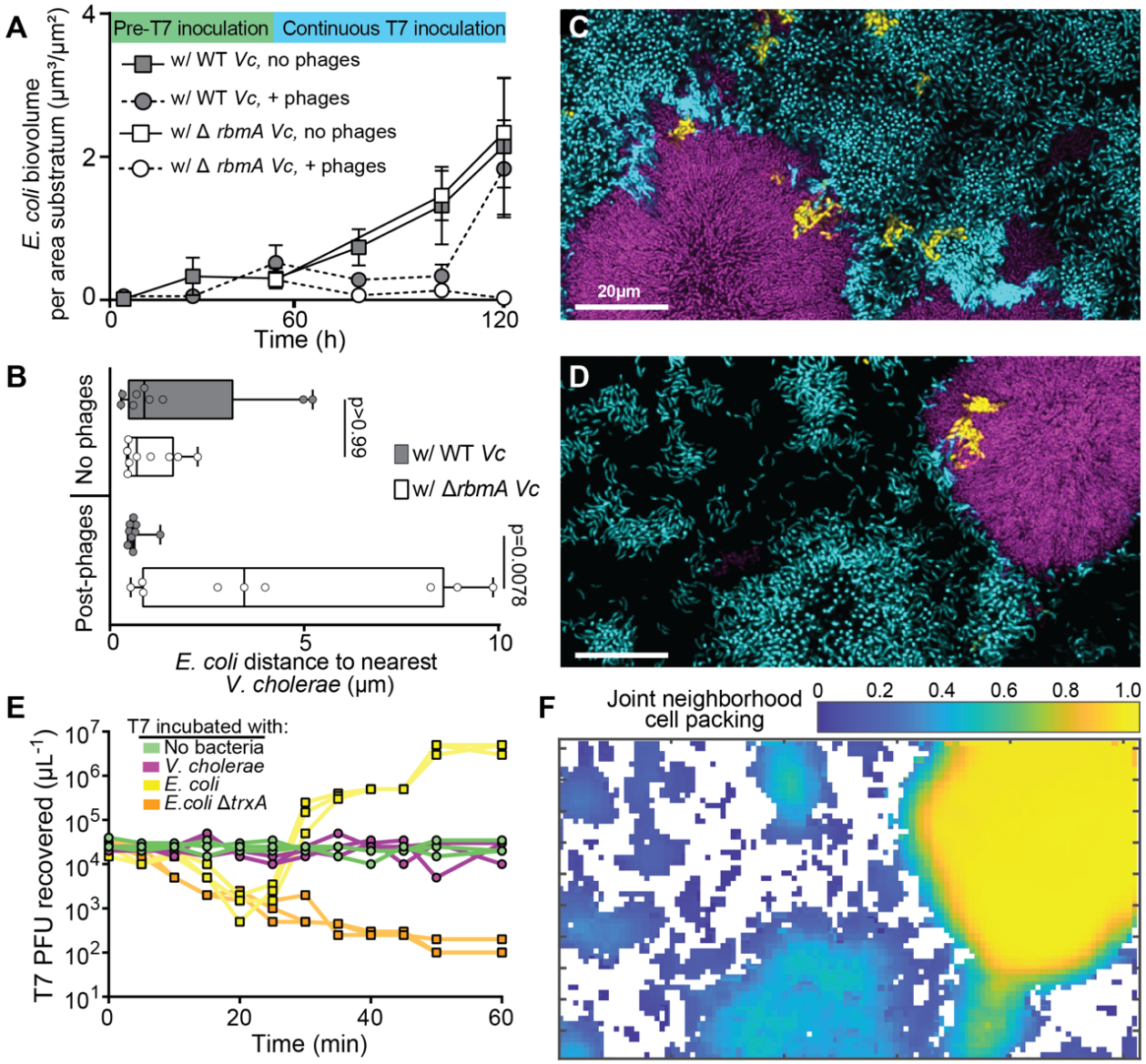

Figure 2. *E. coli* evasion of phages within *V. cholerae* biofilms depends on the cell-cell packing produced by wild type *V. cholerae*. **(A)** *E. coli* biovolume overtime in dual culture conditions with either WT *V. cholerae* or Δ*rbmA V. cholerae* (*n*=3, *n*=4, *n*=6, *n*=6 from top to bottom in legend). **(B)** Average distance between *E. coli* cells and either WT *V. cholerae* or Δ*rbmA V. cholerae* in a triculture condition with or without phage exposure (Wilcoxon paired comparison tests with *n*=9). **(C,D)** Representative images from the triculture condition with *E. coli* (yellow), WT *V. cholerae* (purple), and Δ*rbmA V. cholerae* (cyan) (C) without phage exposure and (D) after phage exposure. **(E)** PFU recovered after incubation of starting T7 phage inoculum with either no bacteria, *V. cholerae*, WT *E. coli*, or Δ*trxA E. coli* over a 60 min time course. Δ*trxA E. coli* allows for T7 phage attachment and genome ejection, but not for phage replication. (**F**) The neighborhood biovolume fraction of the merged biovolumes of both *V. cholerae* genotypes and *E. coli* from (**D**).

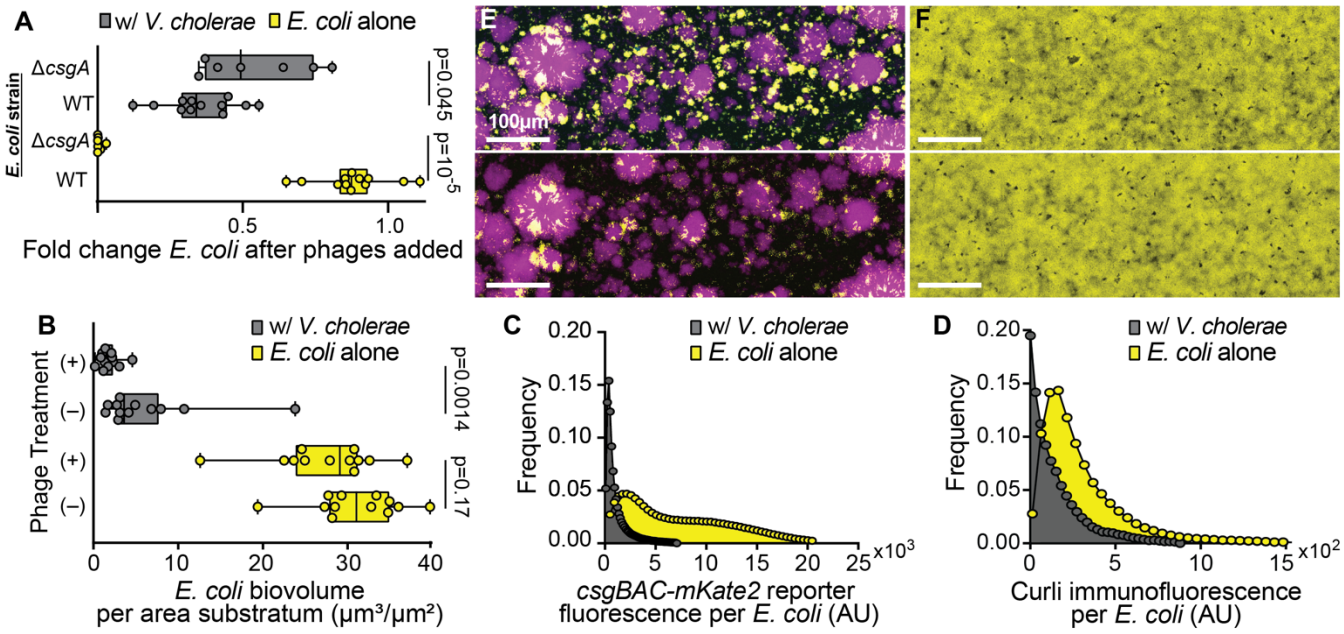

Figure 3. *E. coli* biofilms' normal production of curli matrix protein is interrupted in co-culture with *V. cholerae* to the extent that phage protection is no longer provided by *E. coli* biofilm matrix. **(A)** *E. coli* biovolume normalized to biovolume prior to phage introduction in dual culture and monoculture conditions for both WT *E. coli* and Δ*csgA E. coli* (Mann=Whitney U tests with n=12). **(B)** Total *E. coli* biovolume with and without phage treatments at equivalent time points (Mann-Whitney U tests with n=12). In these experiments, in contrast with Figure 1E, biofilms were grown for longer periods before phage addition such that WT *E. coli* on its own could produce protective curli matrix prior to phage addition. **(C)** Frequency distribution of *csgBAC* transcriptional reporter fluorescence around *E. coli* in monoculture and dual culture conditions. **(D)** Frequency distribution of curli immunofluorescence intensity in proximity to *E. coli* in monoculture and dual culture conditions. **(E)** Dual culture conditions of *E. coli* (yellow) and *V. cholerae* (purple) before phage exposure (top) and after 16 h of continuous phage exposure (bottom). **(F)** Monoculture conditions of *E. coli* before phage exposure (top) and after phage exposure (bottom)

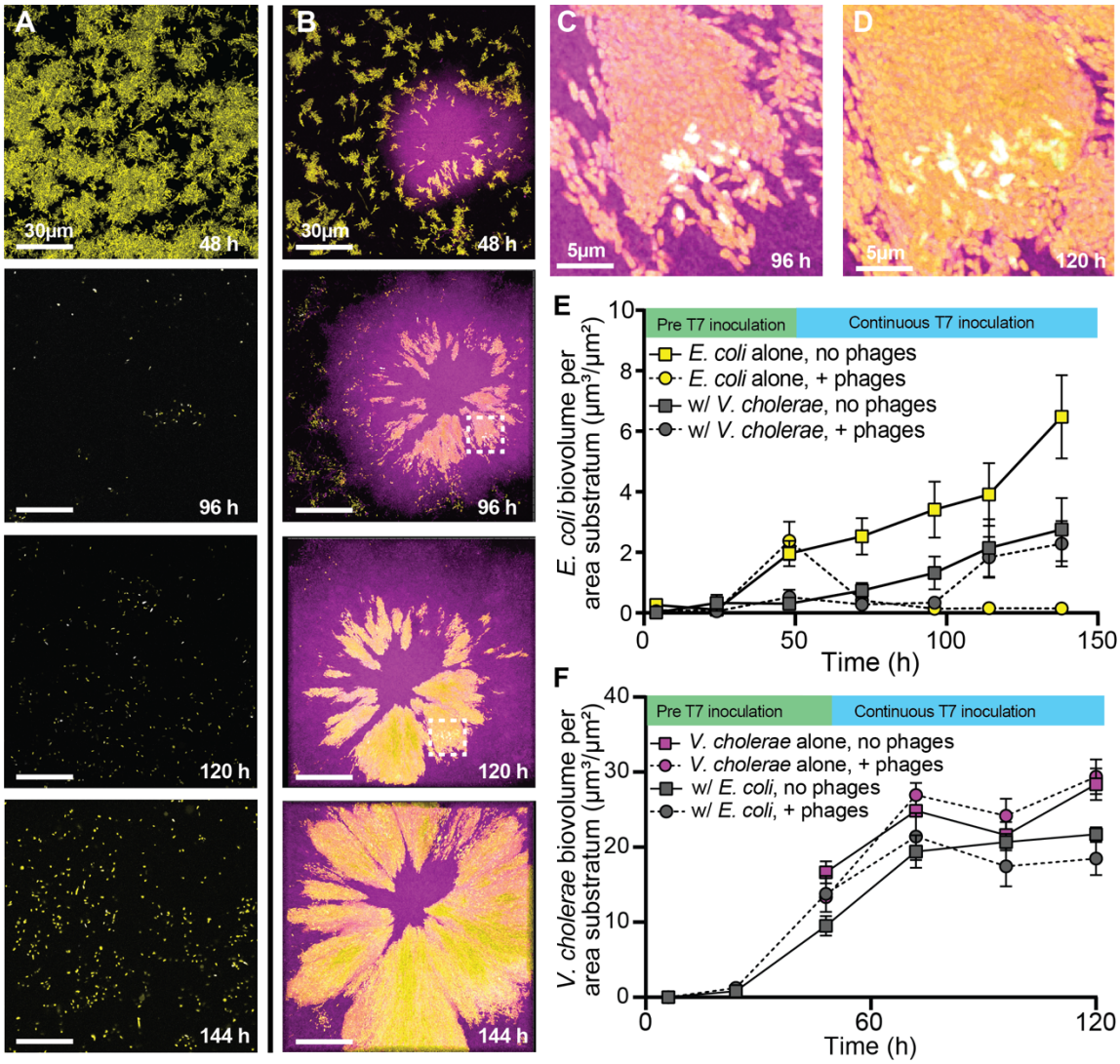

Figure 4. Population dynamics of *E. coli* and *V. cholerae* in monoculture and dual culture conditions, where biofilms grew for 48 h prior to phage exposure, and phage exposure was applied continuously for 96 h thereafter. (**A, B)** Representative images from time course imaging of (A) *E. coli* monoculture and (B) co-culture with *V. cholerae*. **(C, D)** A close-up view of partial *E. coli* phage infection (reporting in cyan/white) within a cluster embedded in a larger colony of *V. cholerae* at (C) 96 h and (D) 120 h. Expanded fields of view in (C) and (D) denoted by checked white boxes in panel B-96 h and B-120 h, respectively. (**E**) *E. coli* population dynamics in monoculture and in co-culture with *V. cholerae*, with and without T7 phage exposure from 48 h onward (*n*=3, *n*=4, *n*=6, *n*=6). (**F**) *V. cholerae* population dynamics in monoculture and in co-culture with *E. coli*, with and without T7 phage exposure from 48 h onward (n=4, n=4, n=8, n=8).

Supplementary Information

Cell group architecture dictates phage exposure in multispecies species biofilms

James B. Winans[1], Benjamin R. Wucher[1], Carey D. Nadell[1]*

[1] Department of Biological Sciences, Dartmouth, Hanover, NH 03755

* Author for correspondence:

carey.d.nadell@dartmouth.edu
78 College St., Rm. 326
Dartmouth, Dept. of Biological Sciences
Hanover, NH 03755

Supplemental Figures

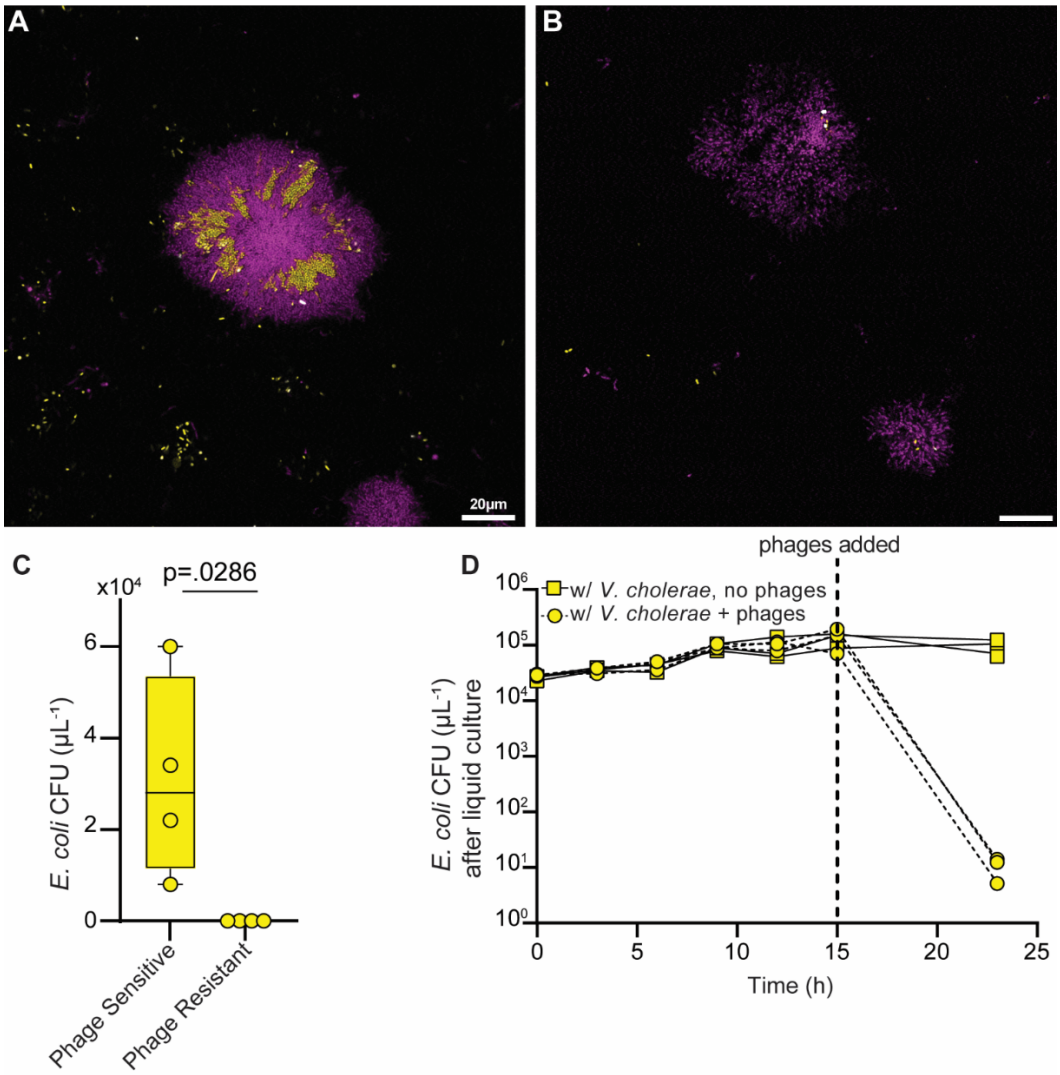

SI Figure S1 – *E. coli* cells that survive T7 phage exposure have not evolved *de novo* phage resistance. (**A**) A co-culture biofilm of *V. cholerae* (purple) and *E. coli* (yellow) after 16 h of phage exposure. (**B**) The same microcolony as (**A**) after heavy disturbance to clear *E. coli* cells out of the chambers to test for phage resistance. (**C**) *E. coli* CFU recovered from co-coculture flow devices when plated without T7 phages (for total counts) or plates saturated with T7 phages (for *de novo* T7-resistant mutants). (**D**) *E. coli* CFU in liquid culture with *V. cholerae* overtime with and without the addition of phages. The addition of *V. cholerae* in shaken liquid culture did not confer protection against phage exposure (n=3).

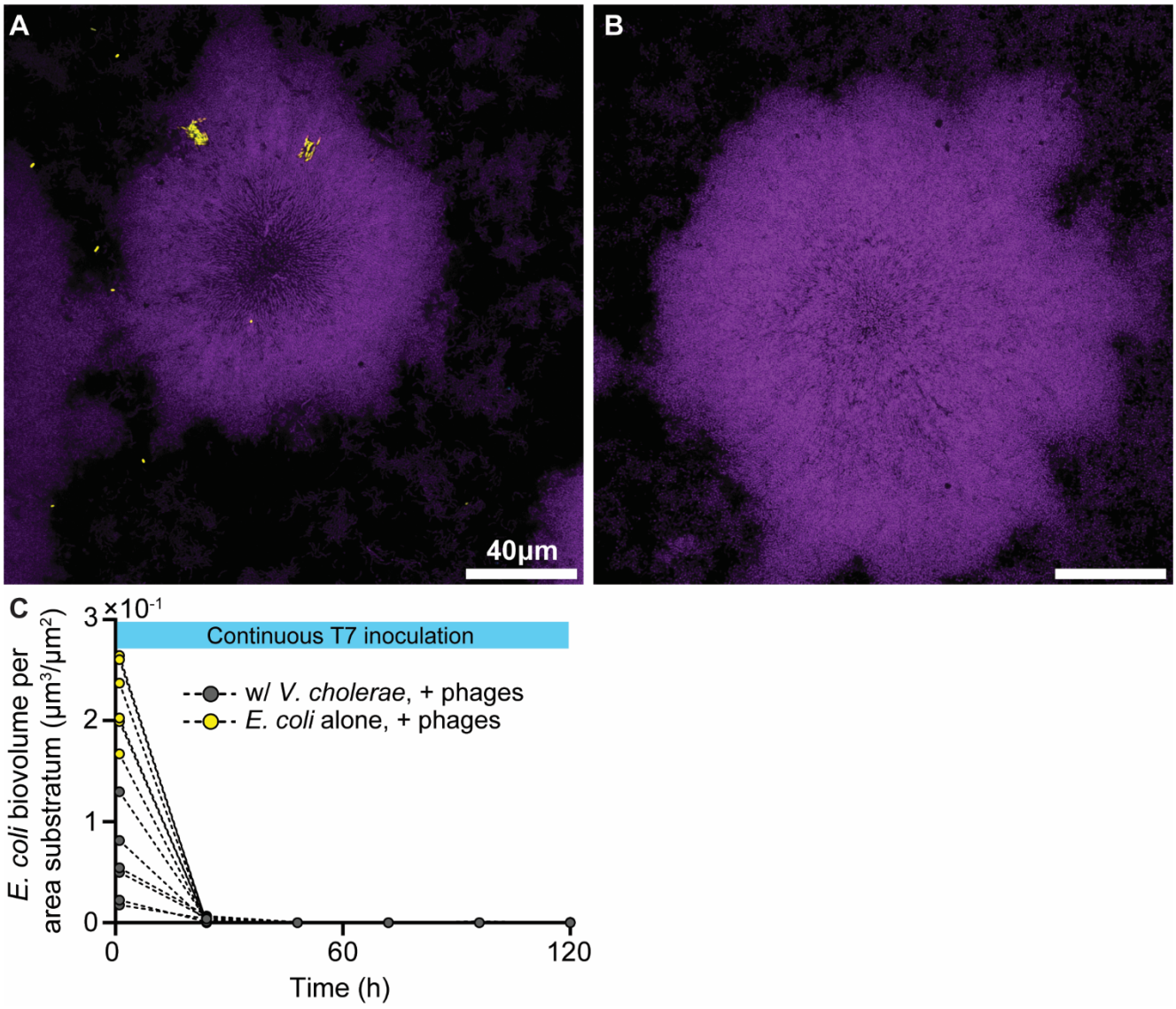

SI Figure S2. *E. coli* does not gain phage exposure protection in co-culture with *V. cholerae* if phages are added to culture from the beginning of biofilm growth. (**A,B**) We surveyed biofilms extensively to see if *E. coli* ever survived when phages were added from the beginning of biofilm growth. Sporadic *E. coli* that had survived phage exposure could be found, but only very rarely. The image in panel (A) is one of only 3 instances out of hundreds of images in which any *E. coli* were found. (**C**) *E. coli* total abundance over time when phages are added continuously from the beginning of biofilm growth either in monoculture or with *V. cholerae* (*n*=12, *n*=12).

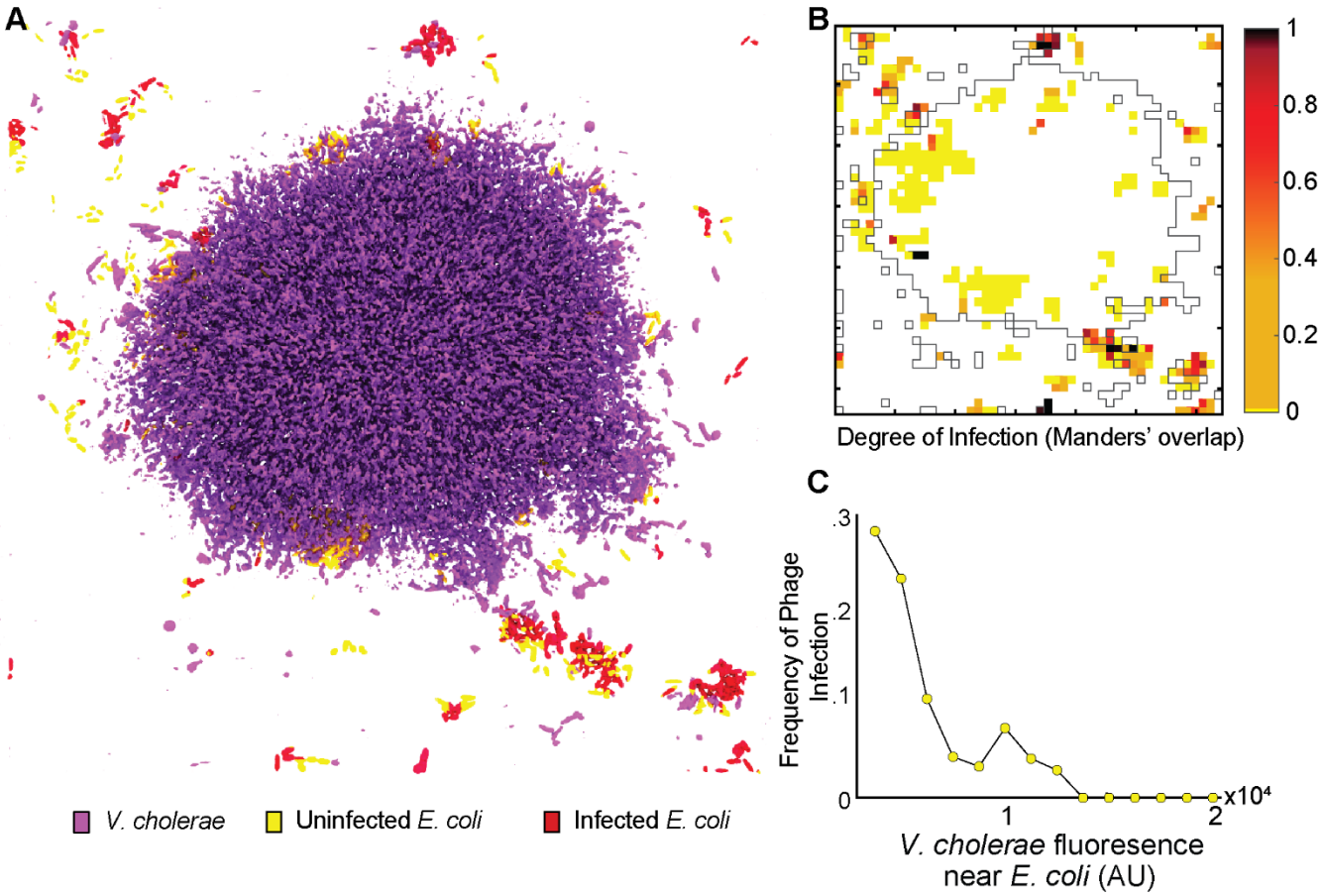

SI Figure S3. *E. coli* cells can evade exposure to λ phages when embedded in *V. cholerae* cell groups in the same manner as observed for T7 phage exposure. (**A**) 3D rendering of *V. cholerae* (purple), *E. coli* (yellow), and *E. coli* with λ phages attached to their cell surface (red). (**B**) Quantification of *E. coli* and λ phage overlap in a top-down view of the biofilm rendered in panel A. *E. coli* clusters within *V. cholerae* biofilms generally evade λ phages, as seen with T7 phages. (**C**) Frequency of phage infection, measured by Mander's overlap coefficient between *E. coli* and λ phage fluorescent signal, as a function of the *V. cholerae* fluorescence shell in proximity to *E. coli*.

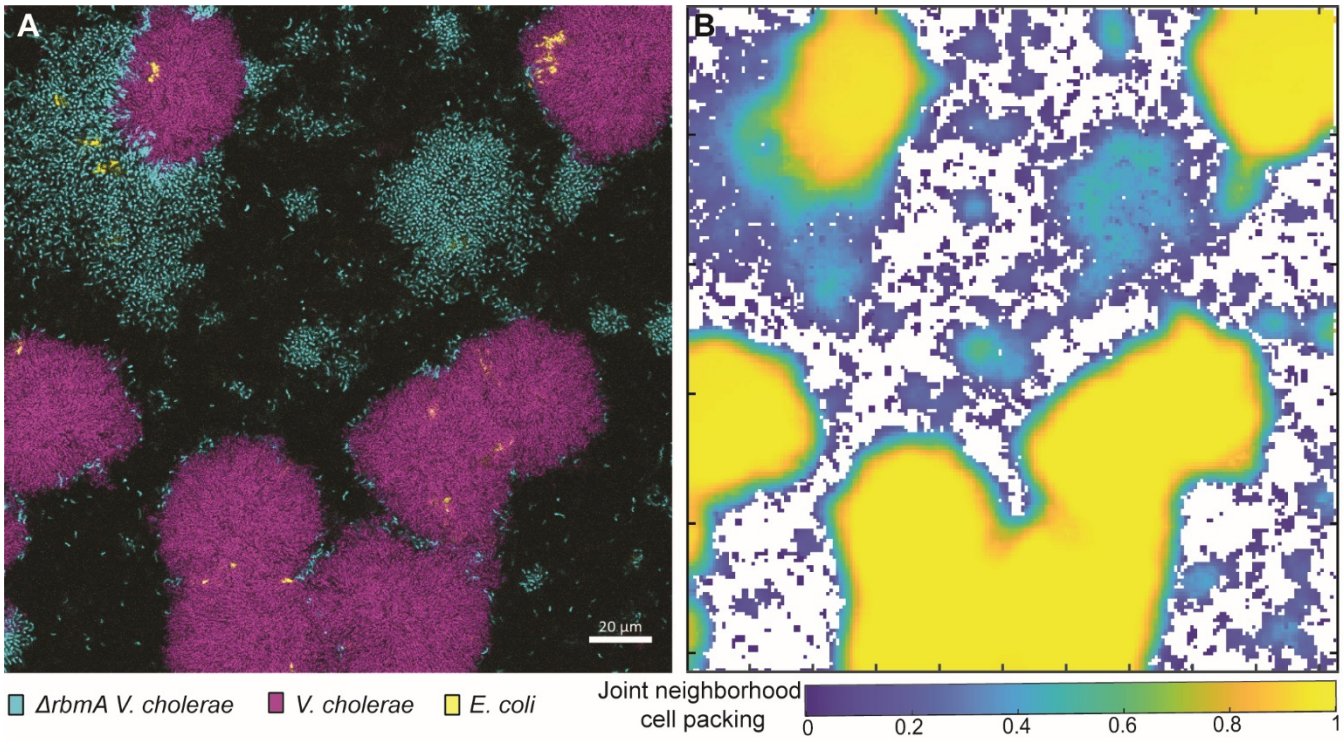

SI Figure S4. Quantification of cell packing for WT *V. cholerae* (purple) and Δ*rbmA V. cholerae* (cyan) in co-culture with *E. coli* (yellow). (**A**) Representative image of a triculture condition of Δ*rbmA V. cholerae, V. cholerae,* and *E. coli*. (**B**) The neighborhood biovolume fraction of the merged biovolumes of both *V. cholerae* genotypes and *E. coli* from (**A**).

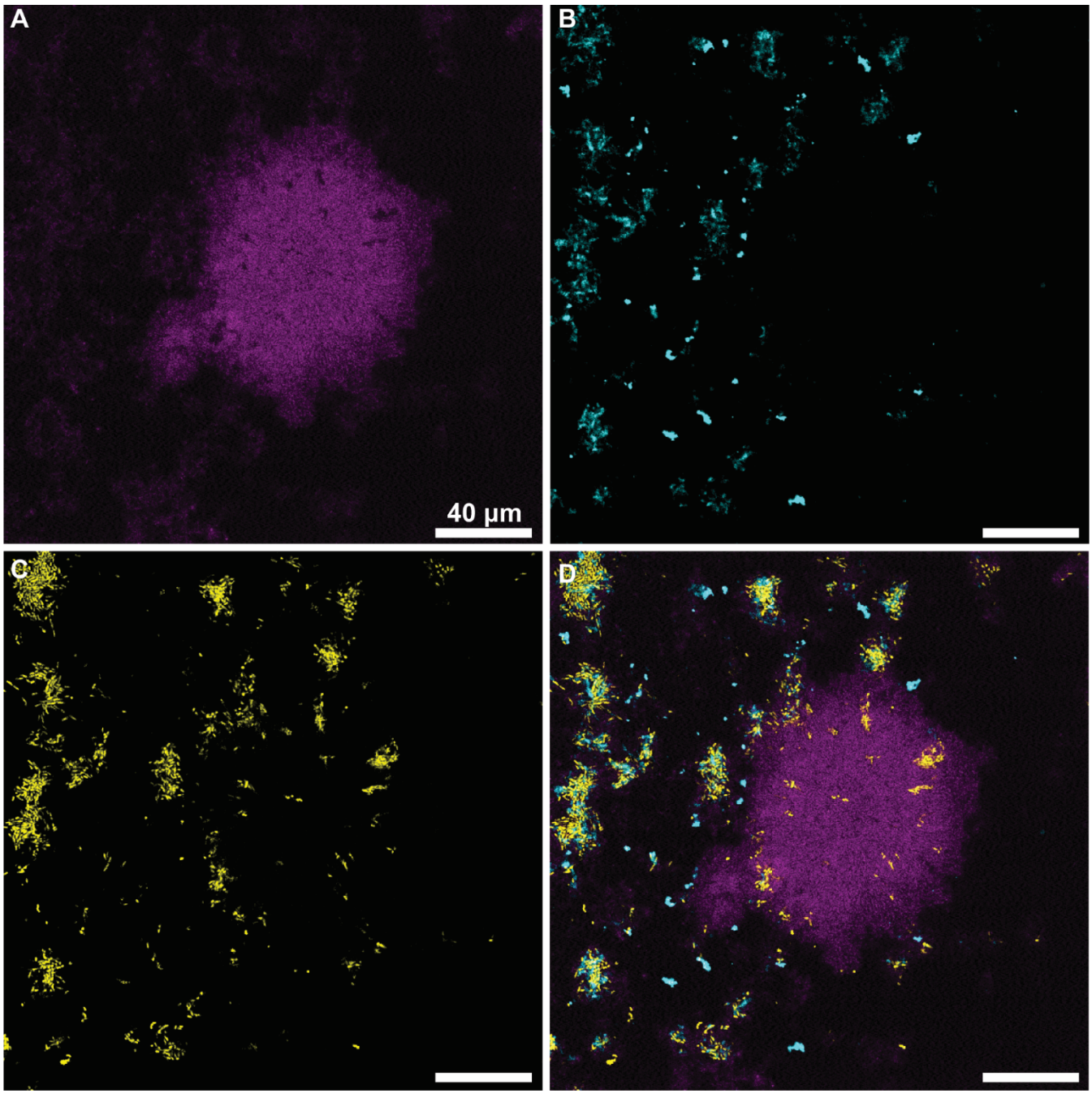

SI Figure S5 Co-culture biofilms exposed to dye-conjugated T7 phages (cyan) show minimal association of phages to *V. cholerae* cell groups (purple) and high T7 localization to *E. coli* (yellow).

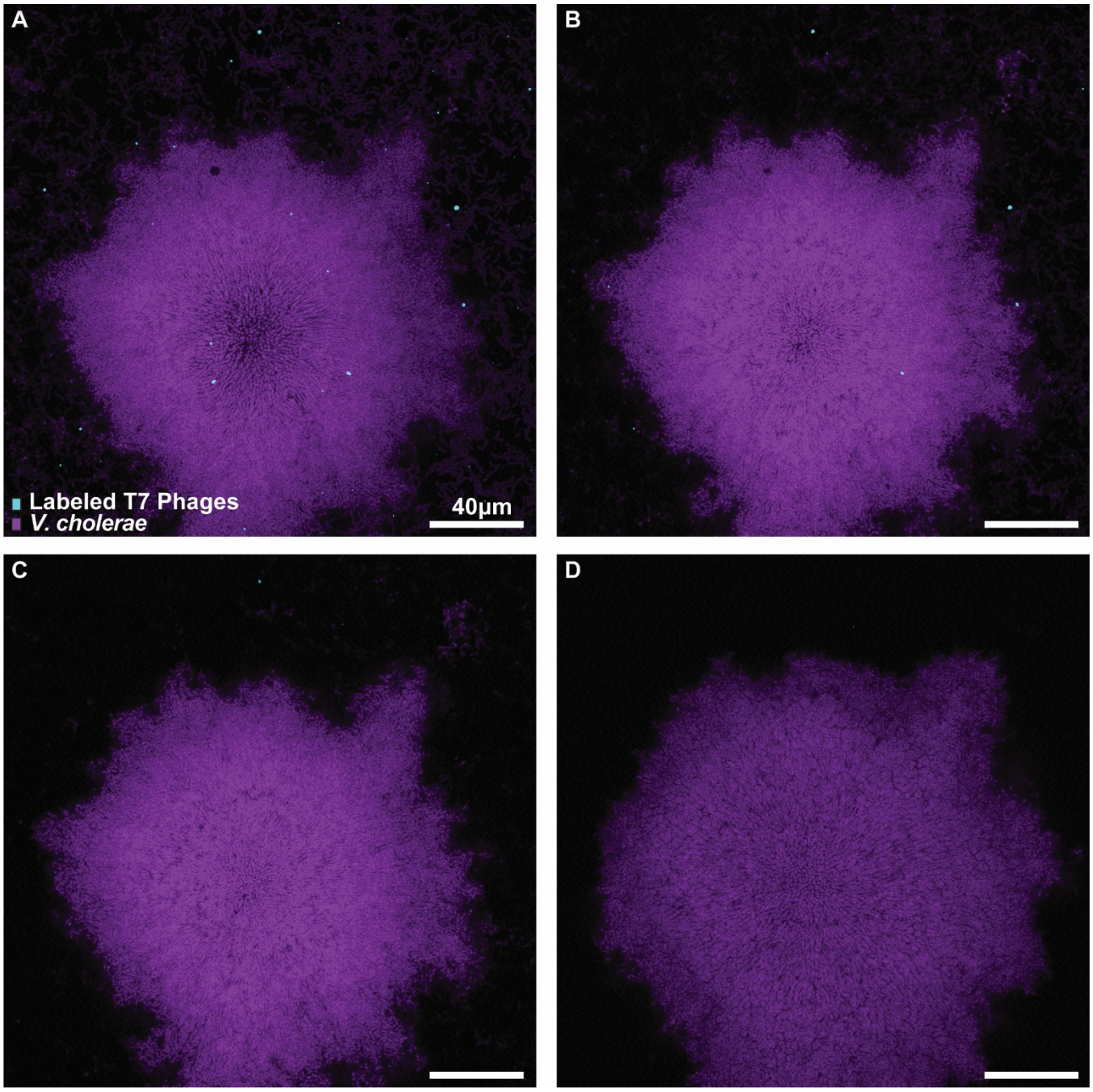

SI Figure S6

V. cholerae biofilms (purple) grown while dye-conjugated T7 phages (cyan) were continously added into the flow devices from the beginning of biofilm growth for 96 h. (**A-D**) Representative image slices taken from a biofilm (A) 1.54μm, (B) 2.70μm, (C) 4.25μm, and (D) 13.90μm above the glass, respectively.

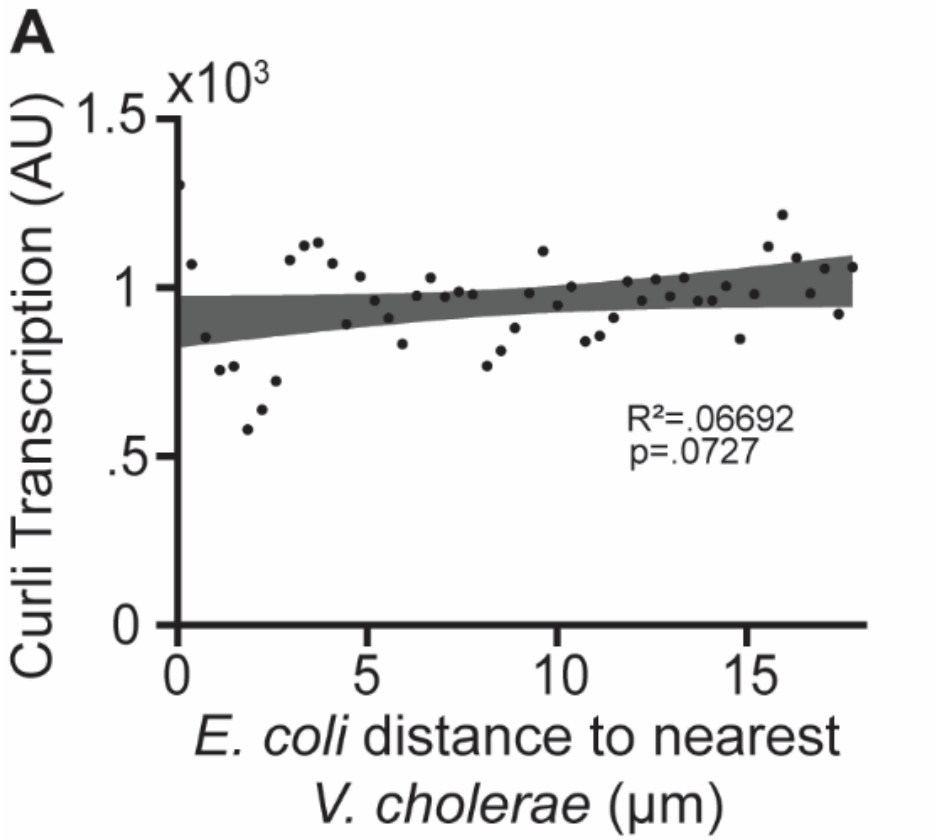

SI Figure S7. Within co-culture flow devices, *E. coli* cells demonstrate similar levels of transcription of *csgBAC* independently of their distance from *V. cholerae*. (**A**) *csgBAC* transcription as a function of distance of *E. coli* cells from the nearest *V. cholerae*.

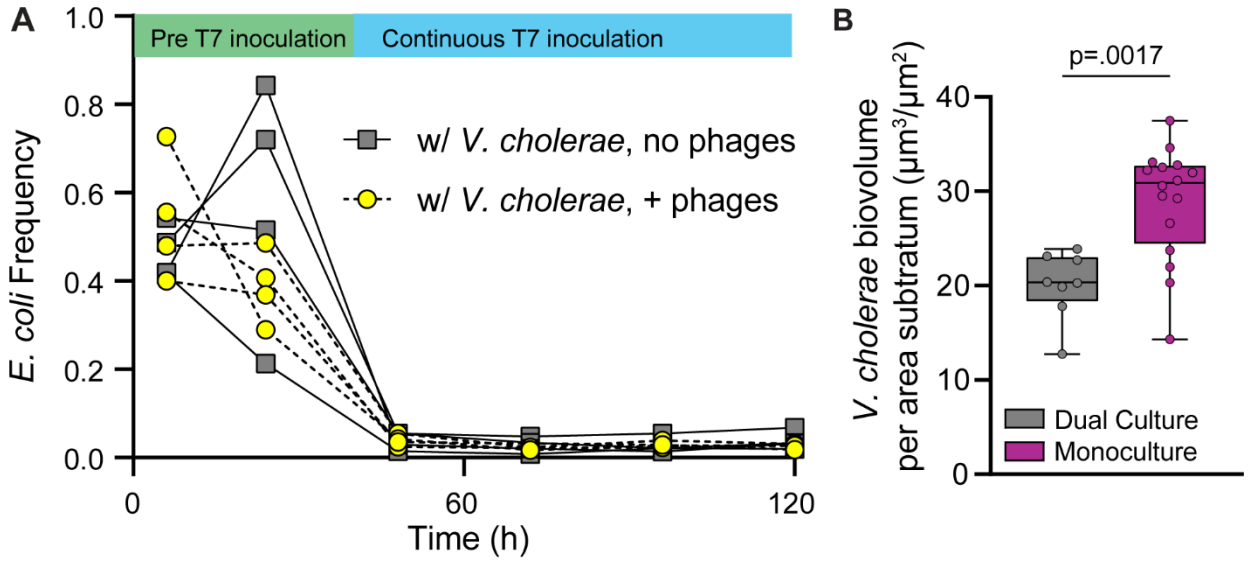

SI Figure S8. *E. coli* and *V. cholerae* compete for space and nutrients with *E. coli* falling to a frequency of 2-5% from a range of starting frequencies. (**A**) *E. coli* frequency in biofilm co-culture with *V. cholerae*, with and without the introduction of phages. (**B**) *V. cholerae* abundance in monoculture and in co-culture with *E. coli*. (Mann-Whitney U-test with n=8 and n=16)

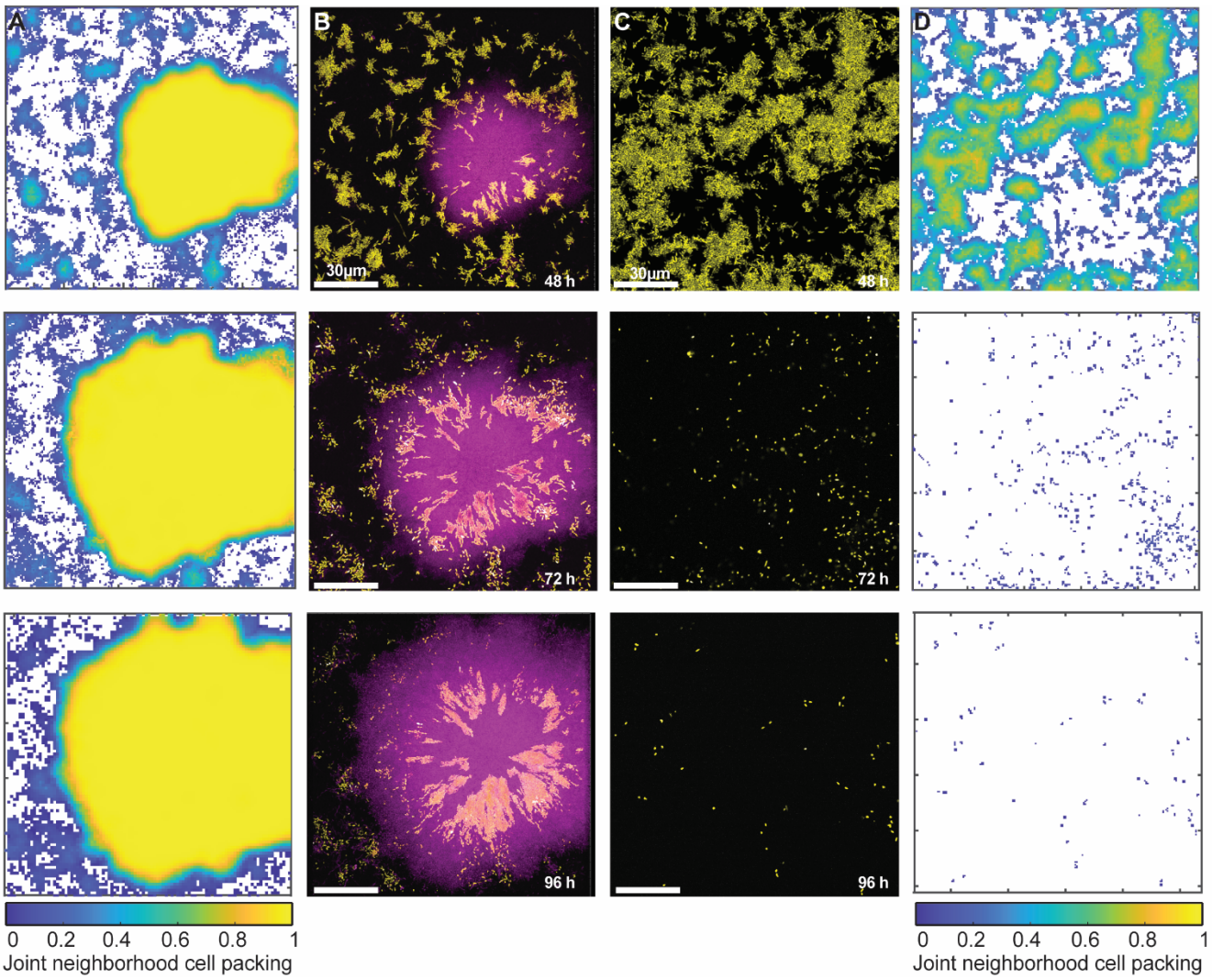

SI Figure S9. *Vibrio cholerae* (purple) biofilm architecture is maintained through time even as *E. coli* (yellow) inclusions continue to grow and expand. (**A**) Heatmaps of the merged neighborhood biovolume fraction for both cell types over the time course experiment reflected in (**B**). (**B**) Dual culture biofilm of *V. cholerae* and *E. coli* overtime, with phages being introduced into this system at 48 h. (**C**) Monoculture of *E. coli* overtime, phages introduced at 48 h. (**D**) Heatmaps of the neighborhood biovolume fraction for the time course reflected in (**D**). *E. coli* biofilms begin at a lower cell density which is abolished by the introduction of phages.